

High-frequency Density Nowcasts of U.S. State-Level Carbon Dioxide Emissions*

Ignacio Garrón
Carlos III University of Madrid
igarron@est-econ.uc3m.es

Andrey Ramos
Carlos III University of Madrid
anramosr@eco.uc3m.es

January 8, 2025

Abstract

Accurate tracking of anthropogenic carbon dioxide (CO₂) emissions is crucial for shaping climate policies and meeting global decarbonization targets. However, energy consumption and emissions data are released annually and with substantial publication lags, hindering timely decision-making. This paper introduces a panel nowcasting framework to produce higher-frequency predictions of the state-level growth rate of per-capita energy consumption and CO₂ emissions in the United States (U.S.). Our approach employs a panel mixed-data sampling (MIDAS) model to predict per-capita energy consumption growth, considering quarterly personal income, monthly electricity consumption, and a weekly economic conditions index as predictors. A bridge equation linking per-capita CO₂ emissions growth with the nowcasts of energy consumption is estimated using panel quantile regression methods. A pseudo out-of-sample study (2009–2018), simulating the real-time data release calendar, confirms the improved accuracy of our nowcasts with respect to a historical benchmark. Our results suggest that by leveraging the availability of higher-frequency indicators, we not only enhance predictive accuracy for per-capita energy consumption growth but also provide more reliable estimates of the distribution of CO₂ emissions growth.

Keywords: *Nowcasting, Quantile regressions, CO₂ emissions, Energy consumption, MIDAS model*

JEL Classification: *C23, C53, Q47, Q50, R10*

*The authors thank Esther Ruiz and Vladimir Rodriguez for their comments and suggestions. Our gratitude extends as well to the attendees of the 44th International Symposium on Forecasting and the Seminario Aleatorio at the Autonomous Technological Institute of Mexico.

1 Introduction

Anthropogenic emissions of carbon dioxide (CO₂) and other greenhouse gases (GHGs) are the primary drivers of climate change since the pre-industrial era (AR6-IPCC, 2021; Jones et al., 2023). The combustion of fossil carbon sources across various sectors—energy, industry, transportation, waste management, and others—combined with land use changes and forestry practices, has led to increased atmospheric CO₂ concentrations, significantly disturbing the Earth’s surface energy balance (Smith et al., 2020; Dong et al., 2021; Friedlingstein et al., 2023). According to the most recent assessment report from the Intergovernmental Panel on Climate Change (IPCC) (AR6-IPCC, 2021), the rise in atmospheric levels of CO₂ and other GHGs attributable to human activities has resulted in a net global average temperature increase of 1.1°C during the industrial period.

The growing concern about the economic and ecological impacts of anthropogenic climate change has rapidly increased the need for policies aimed at reducing CO₂ emissions. Currently, national emissions of CO₂ and other GHGs are extensively regulated by the United Nations Framework Convention on Climate Change (UNFCCC). Parties to the convention are required to set annual CO₂ emission targets in the form of nationally determined contributions under the Paris Agreement (Jones et al., 2023). In this context, accurate tracking anthropogenic CO₂ emissions at national and sub-national levels is essential for the formulation of effective climate policies and for fulfilling long-term international commitments to mitigate climate change impacts. However, in practice, calculation of annual CO₂ emissions requires information on energy consumption that is published approximately 18 months after the end of the reference period. This significant delay poses challenges to a timely and informed decision-making process and underscores the necessity of employing techniques that utilize economic indicators with a more timely publication schedule.

In this paper, we introduce a panel nowcasting methodology to simultaneously obtain high-frequency state-level nowcasts of annual energy consumption and CO₂ emissions growth rate in the United States (U.S.). The set of economic predictors includes the quarterly real personal income from the Bureau of Economic Analysis (BEA), monthly electricity sales from the Energy Information Administration (EIA), and the weekly economic conditions index developed by Baumeister et al. (2024). These indicators are characterized by a higher sampling frequency and a significantly shorter publication delay with respect to the energy consumption data. Building on the recent contribution of Fosten and Nandi (2023b), our approach is implemented in two stages. In the first stage, a panel mixed-data sampling (MIDAS) model is estimated, employing a restricted Almon lag polynomial approximation of the weekly high-frequency component (see, Mogliani and Simoni, 2021; Ferrara et al., 2022; Chuliá et al., 2024), and an unrestricted MIDAS for the monthly and quarterly higher-frequency indicators, as illustrated in Fosten and Nandi (2023b). This strategy is based on Foroni et al. (2015) which indicate that while distributed lag functions, such as the Almon lag functions, are effective for high-frequency indicators, the unrestricted MIDAS performs better for small differences in sampling frequencies. Distin-

guishing our work from [Fosten and Nandi \(2023b\)](#), the use of weekly economic indicator allow us to capture a broader dimension of economic activity potentially enhancing the accuracy of energy consumption predictions. In addition to electricity consumption, this indicator captures labor market conditions, real economic activity, mobility, and expectations. The inclusion of data at weekly frequency is what lends the "high frequency" character to our analysis and enables to produce a most timely monitoring of environmental variables.

In the second stage, a bridge equation linking CO₂ emissions growth and the timely predictions of energy consumption obtained from the panel MIDAS model is estimated using the quantile regression for longitudinal data approach of [Koenker \(2004\)](#). The bridge equation is directly motivated by the procedure implemented by the EIA to compute CO₂ emissions based on energy consumption statistics. The obtained density nowcasts provide important information regarding the distortion of the entire expected CO₂ growth distribution with respect to economic condition changes. Based on the estimates of the conditional quantile function over a discrete number of quantile levels, we estimate the full continuous conditional distribution of CO₂ emissions growth. This approximation allows us to provide not only the expected path of CO₂ growth, but also the uncertainty surrounding the central trajectory, which distinguishes our work from that of [Fosten and Nandi \(2023b\)](#), who employed conditional mean regressions. Following [Adrian et al. \(2019\)](#), we chose to fit a flexible generalized skewed Student's distribution allowing for fat tails and asymmetry. This distribution has also been used with a mixed frequency model in [Ferrara et al. \(2022\)](#) in the context of output growth.

The predictive accuracy of each alternative model is assessed through a pseudo out-of-sample nowcasting study that simulates the real-time release schedule of the data. Several alternatives to combine the higher frequency economic indicators in the panel MIDAS equation are considered. To align closely with the methodology of [Fosten and Nandi \(2023b\)](#), we perform nowcasting exercises that include the quarterly personal income and the monthly electricity sales separately. We also examine models that start with weekly economic indicators and sequentially expand the information set to include monthly and quarterly variables. Additionally, an exercise that directly nowcasts CO₂ emissions growth using annual energy consumption data and all higher-frequency economic indicators, avoiding the bridge step, is conducted. This model mimics the model of [Ferrara et al. \(2022\)](#), in that it introduces variables with different frequencies into a quantile regression model. The nowcasting ability of each alternative model is assessed against the historical mean and quantiles of the nowcasted variables.

A summary of the results of the pseudo-out-of-sample exercise is as follows. Combining predictors with different sampling frequencies is beneficial for nowcasting energy consumption growth. Overall, models that include both the WECI and the monthly electricity sales simultaneously exhibit the best predictive performance across all alternatives. Substantial variation in the performance of the nowcasting exercise between states is obtained, with some states showing improvements of about 60% relative to the historical uncondi-

tional mean benchmark. The gains in predictive accuracy observed in energy consumption growth are translated into the nowcasting of CO2 emissions when using a bridge equation. The best-performing models are again those including the WECI and the monthly electricity sales. A model that directly produces density nowcasts of CO2 growth without relying on a bridge equation shows slightly superior performance, particularly at the lower quantiles.

Our focus on sub-national variables provides a more detailed perspective on environmental degradation, which cannot be captured by aggregated national analyses like those in [Bennedsen et al. \(2021\)](#) or [Jensen \(2021\)](#). Figure 1 illustrates the annual per-capita CO2 emissions levels and growth rates for eight selected states from 1970 to the present. The data reveal considerable heterogeneity in emissions trajectories. For instance, states like California and Ohio show a consistent decrease in CO2 emissions levels, whereas in states like Iowa and Missouri, emissions continued to rise until the mid-2000s. These diverse trajectories reflect the varied policies and technologies implemented across different states, underscoring the significance of analyzing individual units to inform collective environmental goals.

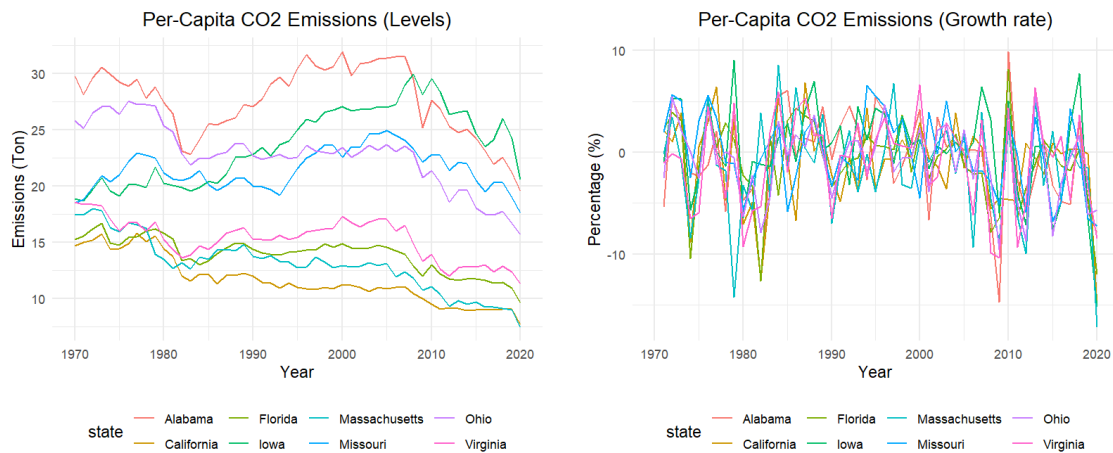


Figure 1: Per-capita CO2 emissions for selected states

Related Literature. This paper is related to the literature on the modeling and forecasting of the relationship between economic activity and CO2 emissions. The seminal contribution by [Grossman and Krueger \(1991\)](#) established the concept of an inverse U-shaped relationship between income and various air pollutants, a relationship now widely referred to as the Environmental Kuznets Curve (EKC). The key idea of the EKC postulates that as income increases, emissions initially rise and then eventually decline. Several mechanisms drive the complex interplay of economic and environmental factors: the scale effect, which suggests that economic growth tends to increase emissions through heightened consumption of natural resources and increased waste production; the composition effect, that implies changes in the economic output mix leading to varying emissions levels; and the technique effect, according to which advances in technology and shifts in the input mix potentially reduce emissions. [Jayachandran \(2022\)](#) provides a recent review of the micro-

empirical literature studying how economic development affects the environment.

From a methodological standpoint, the relationship between economic activity and CO₂ emissions is typically modeled through two approaches: theoretical Integrated Assessment Models (IAMs) and empirical reduced-form econometric models. Our study aligns with the latter. A prevalent method in this domain involves specifying a panel data model that incorporates country and time fixed effects, along with a Almon lag polynomial specification of the income-pollution relationship. However, [Bennedsen et al. \(2023\)](#) highlight several econometric challenges associated with this approach, including functional misspecification, cross-sectional heterogeneity, and structural changes. Semi-parametric panel data models represent one valid alternative to face these challenges by combining parametric fixed effects with a nonparametric regression component, often employing splines or kernels ([Azomahou et al., 2006](#); [Auffhammer and Steinhauser, 2012](#); [Magazzino et al., 2023](#)), as well as neural networks ([Bennedsen et al., 2023](#)).

A complementary interest to modeling is the development of statistical models designed to address practical challenges such as forecasting and nowcasting. For example, [Bennedsen et al. \(2021\)](#) introduce a structural augmented dynamic factor model to analyze the relationship between U.S. CO₂ emissions and a large macroeconomic dataset. This model is utilized to explain, forecast, and nowcast industrial production indices and, consequently, CO₂ emissions through a structural equation. The relevance of nowcasting in this context is underscored by the significant delays in the publication of emissions data. Similarly, [Jensen \(2021\)](#) explores the use of machine learning methods applied to a high-dimensional panel of macroeconomic variables sampled at mixed frequencies. This approach aims to nowcast the yearly growth rate of U.S. CO₂ emissions for the period 2000-2019. Both studies focus on the aggregate level of CO₂ emissions. In contrast, [Fosten and Nandi \(2023b\)](#) adopt a different approach by proposing panel nowcasting methods to provide timely predictions of CO₂ emissions and energy consumption growth across all U.S. states. Their methodology employs a panel MIDAS model that uses quarterly and monthly economic indicators as predictors for energy consumption, coupled with a bridge equation that projects CO₂ emissions based on these energy consumption forecasts.

Our research contributes to the existing literature on CO₂ emissions nowcasting in two ways. First, we expand the methodology established by [Fosten and Nandi \(2023b\)](#) by introducing quantile high-frequency density nowcasts through a panel quantile regression in the bridge equation for CO₂ emissions. This procedure enables the examination of not only the central trajectory of CO₂ emissions, which has been previously investigated in the literature, but also the uncertainty surrounding that trajectory. Indeed, there has been a notable increase in recent years in the focus of policymakers on uncertainty. This is evidenced by the growing body of literature on methodologies for assessing the likelihood of distress scenarios using quantile regressions, which builds on the seminal work of [Adrian et al. \(2019\)](#). Second, we advance the timeliness of our predictions by incorporating high-frequency economic indicators. Unlike [Fosten and Nandi \(2023b\)](#), who limited their analysis to quarterly personal income and monthly electricity sales data, we include

the state-level weekly economic indicator from [Baumeister et al. \(2024\)](#) to predict energy consumption in the panel MIDAS model. This inclusion allows us to capture a wider set of dimensions of economic activity with important capacity to predict energy consumption.

The remainder of the paper is organized as follows. Section 2 describes the data sources and variables used in our analysis. Section 3 outlines the different steps of our nowcasting methodology and the models proposed. The results of the empirical analysis are presented in Section 4. Finally, Section 5 concludes.

2 Data

2.1 State-level CO₂ emissions and energy consumption data

Our primary variable of interest is state-level energy-related CO₂ emissions in the U.S. Data for this variable, sourced from the U.S. EIA, are available annually starting from 1970. Total state CO₂ emissions aggregates emissions from direct fuel use across all sectors, including residential, commercial, industrial, and transportation, as well as from primary fuels consumed for electricity generation. The panel consists of $N = 51$ units, which include the 50 states and the District of Columbia. The publication delay for CO₂ emissions data is approximately two years and three months after the end of the reference year, a notably longer lag compared to other state-level economic data. Our analysis focuses on nowcasting the growth rate of per-capita CO₂ emissions.

Annual energy consumption (EC) data at the state-level is obtained from the State Energy Data System (SEDS) also produced by the EIA. This dataset, available from 1960 onwards, is the main input to compute the state-level CO₂ emissions. In particular, the SEDS collects detailed data on the consumption of coal, natural gas, and petroleum across the different economic sectors. To estimate CO₂ emissions, the EIA applies specific energy content and carbon emission factors to each type of consumed fuel. These factors convert the quantity of fuel used into energy produced and corresponding CO₂ emissions. The calculations are periodically adjusted to reflect changes in fuel composition and new scientific findings. Regarding timeliness of the data, the publication lag of energy consumption is approximately 18 months, considerably shorter than that for CO₂ emissions. As with CO₂ emissions, we focus on the growth rate of per-capita energy consumption.

2.2 Higher-frequency economic indicators

State-level economic indicators are available at higher frequency and are published in a more timely fashion than CO₂ emissions or energy consumption. Concretely, quarterly real and per-capita personal income (PI) is obtained from the BEA since 1950 and features a publication lag of approximately three months. Monthly electricity consumption (ELEC), computed as total electricity sales to end-users across all U.S. states, is published by the EIA since 1990 with a publication lag of about two months following the end of the reference month. For the analysis, we consider the year-on-year log difference of both variables.

Both variables, PI and ELEC, are employed as predictors in the analysis of [Fosten and Nandi \(2023b\)](#). We extend the scope of the analysis by including the weekly economic conditions index (WECI) developed by [Baumeister et al. \(2024\)](#). Starting in 1987, the WECI is derived from a mixed-frequency dynamic factor model that integrates a wide set of weekly, monthly, and quarterly economic variables. It encompasses a comprehensive range of economic dimensions, including labor market indicators, household spending, real economic activity, mobility, financial indicators, and expectations. The publication lag is approximately one month, as indicated on the author’s website. The high-frequency nature of our nowcasting approach stems from the use of this variable.

3 Nowcasting Methodology

Our nowcasting approach is implemented in two stages. In the first stage, we propose a panel MIDAS model to predict energy consumption growth, utilizing quarterly, monthly, and weekly economic predictors. A restricted Almon lag polynomial approximation of the weekly high-frequency component is employed, as outlined in [Mogliani and Simoni \(2021\)](#), [Ferrara et al. \(2022\)](#), and [Chuliá et al. \(2024\)](#). This is combined with an unrestricted MIDAS model for the monthly and quarterly indicators, as in [Fosten and Nandi \(2023b\)](#). In the second stage, we employ a bridge equation to generate predictions for CO2 emissions growth, using the first-stage nowcasts of energy consumption growth as the predictor variable. Distinctively from [Fosten and Nandi \(2023b\)](#), we move beyond the conditional-mean predictions framework and produce density forecasts adopting the panel quantile regressions approach of [Koenker \(2004\)](#). Out-of-sample density nowcasts are obtained for the period 2009 to 2018, and their performance both on aggregate and individual levels are evaluated using different metrics. The subsequent subsections provide a detail each of these steps. A note on notation: we use bold letters to refer to vectors and matrices.

3.1 Nowcasting energy consumption growth using a panel MIDAS model

As explained earlier, to compute state-level CO2 emissions, the EIA uses the energy content and carbon emission factors for each consumed fuel type, converting fuel use into energy produced and CO2 emitted. These calculations are periodically updated by changes in fuel composition and scientific advances in terms of energy efficiency. Energy consumption data, published with an 18-month lag, is timelier than CO2 emissions data. Thus, we first nowcast energy consumption growth.

Consider the following general model,

$$\underbrace{c_{i,t}}_{\text{Annual}} = g_v(c_{i,t-d_v}, \underbrace{\mathbf{x}_{i,t-\frac{q_v}{4}}^{(q)}}_{\text{Quarterly}}, \underbrace{\mathbf{z}_{i,t-\frac{m_v}{12}}^{(m)}}_{\text{Monthly}}, \underbrace{\mathbf{w}_{i,t-\frac{w_v}{52}}^{(w)}}_{\text{Weekly}}) + u_{i,t}, \quad (1)$$

where $c_{i,t}$ is the annual growth rate of per-capita energy consumption at state i , $i = 1, 2, \dots, N$, and year t , $t = 1, 2, \dots, T$. We define $\mathbf{x}_{i,t-\frac{q_v}{4}}^{(q)}$ as a (4×1) vector of quarterly PI

growth lags, $\mathbf{z}_{i,t-\frac{m_v}{12}}^{(m)}$ as a (12×1) vector of monthly ELEC growth lags, and $\mathbf{w}_{i,t-\frac{w_v}{52}}^{(w)}$ as a (52×1) high-frequency vector of WECEI growth lags, which are observed $q = 4$, $m = 12$, $w = 52$ times between year $t - 1$ and t . We denote v as the calendar date of prediction. The available lag of the dependent variable is represented by d_v , while for the quarterly, monthly, and weekly predictors are denoted by q_v , m_v , and w_v , respectively. The target function $g_v(\cdot)$ maps our covariates for a given calendar v , and $u_{i,t}$ is a zero mean random error.

The general nowcasting equation is,

$$\widehat{c}_{i,t} = \widehat{g}_v(c_{i,t-d_v}, \mathbf{x}_{i,t-\frac{q_v}{4}}^{(q)}, \mathbf{z}_{i,t-\frac{m_v}{12}}^{(m)}, \mathbf{w}_{i,t-\frac{w_v}{52}}^{(w)}), \quad (2)$$

where $\widehat{g}_v(\cdot)$ is the predicted target function for the given calendar date of prediction v . As is common in the nowcasting literature, the information contained in v is set to reflect the release schedule of the variables in real time. This allows for the generation of multiple nowcasts and backcasts for each period under consideration. This approach enables an assessment of how the performance of our model changes as new information is incorporated into the nowcasting model; see, for instance, [Giannone et al. \(2008\)](#); [Bańbura et al. \(2013\)](#); [Fosten and Nandi \(2023b\)](#).

It should be noted that the number of parameters in this specification is considerable large, particularly in the case of the weekly variable. This may give rise to a proliferation of parameters, which could render standard regression procedures invalid. In the following section, we present our MIDAS framework, which we employed to estimate the aforementioned regression.

3.2 MIDAS setup

Let us consider a linear panel MIDAS model for $g_v(\cdot)$:

$$c_{i,t} = \alpha_i + \phi_v c_{i,t-d_v} + \mathcal{B}(L^{q_v/q}, \boldsymbol{\beta}_q) x_{i,t}^{(q)} + \mathcal{B}(L^{m_v/m}, \boldsymbol{\beta}_m) z_{i,t}^{(m)} + \mathcal{B}(L^{w_v/w}, \boldsymbol{\theta}_w) w_{i,t}^{(w)} + u_{i,t}, \quad (3)$$

and,

$$\begin{aligned} \mathcal{B}(L^{q_v/q}, \boldsymbol{\beta}_q) x_{i,t}^{(q)} &= \beta_{1,q} x_{i,t-\frac{q_v}{4}}^{(q)} + \beta_{2,q} x_{i,t-\frac{q_v-1}{4}}^{(q)} + \beta_{3,q} x_{i,t-\frac{q_v-2}{4}}^{(q)} + \beta_{4,q} x_{i,t-\frac{q_v-3}{4}}^{(q)}, \\ \mathcal{B}(L^{m_v/m}, \boldsymbol{\beta}_m) z_{i,t}^{(m)} &= \beta_{1,m} z_{i,t-\frac{m_v}{12}}^{(m)} + \beta_{2,m} z_{i,t-\frac{m_v-1}{12}}^{(m)} + \beta_{3,m} z_{i,t-\frac{m_v-2}{12}}^{(m)} + \dots + \beta_{1,m} z_{i,t-\frac{m_v-11}{12}}^{(m)}, \\ \mathcal{B}(L^{w_v/w}, \boldsymbol{\theta}_w) w_{i,t}^{(w)} &= \sum_{c=0}^{C_w-1} \sum_{l=0}^p \tilde{B}(c; \boldsymbol{\theta}_w) L^{c/w} w_{i,t-w_v}^{(w)}, \end{aligned}$$

where the lag coefficients in $\mathcal{B}(L^{q_v/q}, \boldsymbol{\beta}_q)$, $\mathcal{B}(L^{m_v/m}, \boldsymbol{\beta}_m)$, and $\mathcal{B}(L^{w_v/w}, \boldsymbol{\theta}_w)$ are parameterized as a function of a low dimensional vector of parameters. Here, α_i represents the individual fixed effects, ϕ is the autoregressive parameter, and $u_{i,t}$ is a zero-mean random error term.

As noted in [Equation 3](#), no restrictions are placed on the quarterly and monthly vari-

ables, while an Almon lag polynomial is applied to the weekly indicator. Specifically, $\tilde{B}(c; \boldsymbol{\theta}_w)$ is a weighting function, normalized to sum up to 1, which depends on a vector of parameters $\boldsymbol{\theta}_w$ and lag-order c . For the Almon-lags choice, $\tilde{B}(c; \boldsymbol{\theta}_w) = \sum_{l=0}^p \theta_{l,w} c^l$, where $\boldsymbol{\theta}_w := (\theta_{0,w}, \theta_{1,w}, \dots, \theta_{p,w})'$. Also, it is desirable to further consider restrictions on the value and slope of the lag polynomial $\tilde{B}(c; \boldsymbol{\theta}_w)$. In particular, by imposing $\tilde{B}(C_w - 1; \boldsymbol{\theta}_w) = 0$ and $\nabla_c \tilde{B}(C_w - 1; \boldsymbol{\theta}_w|_{c=C_w-1}) = 0$, we consider a lag structure with good economic properties, as it slowly decays towards zero (see [Mogliani and Simoni, 2021](#)).

Under the so-called "direct-method", [Equation 4](#) can be re-parameterized as:

$$c_{i,t} = \alpha_i + \phi c_{i,t-d_v} + \underbrace{\mathbf{x}_{i,t-\frac{q_v}{4}}^{(q)'} \boldsymbol{\beta}_q}_{\text{unrestricted}} + \underbrace{\mathbf{z}_{i,t-\frac{k_v}{12}}^{(m)'} \boldsymbol{\beta}_m}_{\text{unrestricted}} + \underbrace{\tilde{\mathbf{w}}_{i,t-\frac{w_v}{52}}^{(w)'} \hat{\boldsymbol{\theta}}_w}_{\text{Almon}} + u_{i,t}. \quad (4)$$

where $\boldsymbol{\beta}_q$ is a (4×1) vector, $\boldsymbol{\beta}_m$ is a (12×1) vector, and $\tilde{\boldsymbol{\theta}}_w^{(w)}$ is a vector featuring $(p+1-r \times 1)$ parameters. The vector $\tilde{\mathbf{w}}_{i,t} := \mathbf{Q}_w \mathbf{w}_{i,t}$ with size $(p+1-r \times 1)$ are linear combinations of the WECI lags, and \mathbf{Q}_w is a $(p+1-r \times C_w)$ polynomial weighting matrix defined accordingly. In our application, which we consider a third-degree Almon lag polynomial ($p = 3$) with two end-point restrictions $r = 2$, so that the number of parameters of the high-frequency indicator is reduced substantially to $p+1-r = 2$; see [Ferrara et al. \(2022\)](#) and [Chuliá et al. \(2024\)](#) who consider the same parametrization. As the model is linear in parameters, [Equation 4](#) can be estimated by panel least squares (see, [Fosten and Nandi, 2023b](#); [Feroni et al., 2015](#)). In terms of consistency, MIDAS models require that lag order of $c_{i,t}$ and the lag polynomials are sufficiently large to make $u_{i,t}$ white noise (see [Ghysels et al., 2006](#); [Feroni et al., 2015](#)).

Thus, the nowcasting equation becomes,

$$\hat{c}_{i,t} = \hat{\alpha}_i + \hat{\phi} c_{i,t-d_v} + \mathbf{x}_{i,t-\frac{q_v}{4}}^{(q)'} \hat{\boldsymbol{\beta}}_q + \mathbf{z}_{i,t-\frac{k_v}{12}}^{(m)'} \hat{\boldsymbol{\beta}}_m + \tilde{\mathbf{w}}_{i,t-\frac{w_v}{52}}^{(w)'} \hat{\boldsymbol{\theta}}_w. \quad (5)$$

The combination of frequencies in [Equation 5](#) offers the advantage of considering all the information in a single regression. Our strategy is based on the montecarlo results of [Feroni et al. \(2015\)](#), which indicate that while distributed lag functions, such as the Almon lag functions, are effective for high-frequency indicators, whereas the unrestricted function performs better for small differences in sampling frequencies. Also, similar approaches has been implemented and demonstrated to enhance accuracy in the literature, as evidenced by the works of [Ferrara et al. \(2022\)](#) and [Carriero et al. \(2022\)](#). To this end, we employ a restricted Almon lag polynomial for the weekly high-frequency indicator [Mogliani and Simoni \(2021\)](#), while allowing for an unrestricted polynomial for the monthly and quarterly higher-frequency indicators, as illustrated in [Fosten and Nandi \(2023b\)](#).

3.3 Nowcasting CO2 emissions growth using a bridge equation

CO2 emissions growth is the main target variable in our analysis. Timely predictions of this variable are produced via a bridge equation linking energy consumption and CO2 emissions. Let $\hat{c}_{v,i,t}$ the predicted value of $c_{i,t}$ for state i at year t and nowcast time v .

The conditional mean forecast panel bridge equation with a multi-factor error structure, adopted from [Fosten and Nandi \(2023b\)](#), is given by:

$$e_{i,t} = \gamma_i + \rho e_{i,t-g_v} + \delta \widehat{c}_{v,i,t} + \boldsymbol{\lambda}' \mathbf{f}_{t-d_v} + \epsilon_{i,t}, \quad (6)$$

where $e_{i,t}$ denotes the per-capita CO2 emissions growth, d_v is the last available lag of $e_{i,t}$, \mathbf{f}_{t-d_v} are unknown common factors with loading vector $\boldsymbol{\lambda}$. In a similar fashion to [Fosten and Nandi \(2023b\)](#), the factors estimates are obtained by taking an average of the covariates, such that $\mathbf{f}_t = [\bar{e}_{i,t-d_v}, \bar{c}_{i,t-d_v}]'$. The parameters γ_i , ρ , δ and $\boldsymbol{\lambda}$ capture the fixed effects, the autoregressive coefficient, the effect of EC growth prediction from the first step, and the factors coefficients, respectively. Once the common factors are obtained, the model can be estimated using panel least squares (see, [Fosten and Nandi, 2023a](#)).

Our main contribution to this framework is to produce density nowcasts for $e_{i,t}$ using the quantile regression for longitudinal data proposed by [Koenker \(2004\)](#). The conditional quantile of $e_{i,t}$ is modeled as:

$$Q_{e_{i,t}}(\tau | e_{i,t-g_v}, \widehat{c}_{v,i,t}, \mathbf{f}_t) = \gamma_i(\tau) + \rho(\tau) e_{i,t-g_v} + \delta(\tau) \widehat{c}_{v,i,t} + \boldsymbol{\lambda}'_v(\tau) \mathbf{f}_{t-d_v}, \quad (7)$$

where $\tau = 0.25, 0.50, 0.75$ denotes the quantile level. Consequently, our framework considers the effect of our covariates on the conditional distribution of $e_{i,t}$. [Koenker \(2004\)](#) proposes the estimation of Equation 7 employing ℓ_1 regularization methods. As [Koenker \(2004\)](#) points out, the introduction of individual fixed effects may result in a notable increase in the variability of estimates of other covariate effects. The application of regularization of these individual effects towards a common value, can assist in modifying this inflation effect. Nevertheless, determining the optimal degree of shrinkage presents a significant practical challenge when dealing with multiple calendar dates.¹

We consider another alternative to produce high-frequency density nowcasts of the growth rate of per-capita CO2 emissions without relying on the bridge equation, in the spirit of [Ferrara et al. \(2022\)](#). This alternative directly predicts the conditional quantile function of $e_{i,t}$, directly conditioning on the full set of weekly, monthly, and quarterly predictors. Adapting the equation in [Ferrara et al. \(2022\)](#) to a panel data framework, the estimated model is given by:

$$Q_{e_{i,t}}(\tau | e_{i,t-g_v}, \mathbf{x}_{i,t-\frac{q_v}{4}}^{(q)}, \mathbf{z}_{i,t-\frac{k_v}{12}}^{(m)}, \tilde{\mathbf{w}}_{i,t-\frac{w_v}{52}}^{(w)}, \mathbf{f}_t) = \gamma_i(\tau) + \rho(\tau) e_{i,t-g_v} + \mathbf{x}_{i,t-\frac{q_v}{4}}^{(q)'} \widehat{\boldsymbol{\beta}}_q(\tau) + \mathbf{z}_{i,t-\frac{k_v}{12}}^{(m)'} \widehat{\boldsymbol{\beta}}_m(\tau) + \tilde{\mathbf{w}}_{i,t-\frac{w_v}{52}}^{(w)'} \widehat{\boldsymbol{\theta}}_w(\tau) + \lambda(\tau) \mathbf{f}_{t-d_v}. \quad (8)$$

Based on these estimates, a full continuous conditional distribution is estimated as in [Adrian et al. \(2019\)](#) and [Ferrara et al. \(2022\)](#). We choose to fit a generalized skewed Student's t distribution ([Azzalini and Capitanio, 2003](#)), which depends on four parameters associated to location, scale, fatness, and shape. These parameters are obtained through a

¹In the context of our application, we have set this parameter equal to one, and the resulting nowcasting exercise has yielded satisfactory results.

quantile matching approach aiming at minimizing the squared distance between the estimated discrete conditional quantiles and the corresponding quantiles of the skewed Student’s distribution, as in [Adrian et al. \(2019\)](#). This procedure is flexible to accommodate fat tails and asymmetry potentially present in the context of our application.

3.4 Competing models

Table 1 illustrates the various specifications considered in our empirical exercise. As simple benchmarks, we consider the historical mean and a one-lag autoregressive (AR) model, as in [Fosten and Nandi \(2023a\)](#). In addition, models AR-Q and AR-M, which include only the monthly and quarterly variables, respectively, are defined as in [Fosten and Nandi \(2023b\)](#). The rest of the models include the weekly information (AR-W), jointly with the monthly (AR-W-M), and all variables sampled at different frequencies (AR-W-M-Q). Finally, the direct AR-W-M-Q considers the direct quantile nowcast approach as in [Equation 8](#).

Table 1: Competing models

Model	Information considered for the bridge model
Benchmark model	Historical mean
AR	Autoregressive model with order 1
AR-M	AR + monthly variable (UMIDAS)
AR-Q	AR + quarterly variable (UMIDAS)
AR-W	AR + weekly variable (Almon MIDAS)
AR-W-M	AR + monthly (UMIDAS) + weekly variables (Almon MIDAS)
AR-W-M-Q	AR + monthly and quarterly (UMIDAS) + weekly variables (Almon MIDAS)
Direct AR-W-M-Q	Defined as in Equation 8 .

3.5 Out-of-sample exercise

To maintain comparability with [Fosten and Nandi \(2023b\)](#), we generate out-of-sample nowcasts for the period 2009 to 2018 across the 50 individual states. The estimation period starts from 1990 and it considers an expanding window. For each year in the evaluation period, we use a weekly calendar to make multiple nowcast and backcast updates on different dates, v . This approach aims to replicate the ragged edge in the data, emulating real-time releases. For each data release, we incorporate the new data lag available, adjust the lag structure of the model, re-estimate the model, and obtain energy consumption and CO2 predictions. This enables us to observe the behavior of our predictions as we incorporate additional information as it becomes available.

A distinctive feature of our proposed calendar is its consideration of a weekly calendar. Our calendar is based on [Fosten and Nandi \(2023b\)](#), and is extended to accommodate WECI information. Table 2 illustrates the full information flow for the year 2021 as an illustrative example. As the year progresses, new observations of WECI are incorporated each week, new observations of ELEC are added each month, and new observations of PI are included each quarter. Beginning from the backcasting period, WECI data is incorporated until the end of week 4 (January), at which point all data up to December of the previous

year are available. Subsequently, the nowcasting period is initiated, where weekly data from the current year is incorporated at every week. Monthly data for the current year is introduced from week 8 (March), while quarterly data for the PI is added from week 21 (June). Annual data for previous years (specifically 2018 and 2019) for CO2 and EC are incorporated in week 8 (June) and week 20 (March), respectively. In total, we consider 48 weeks for the prediction period.

For the EC growth bridge model, the prediction accuracy is evaluated by comparing the average root mean squared forecast error (RMSFE) of the nowcast model with those of a benchmark consisting of the historic average using the data available at the time of the nowcast. The RMSFE is tracked across multiple nowcast dates, v , and is defined as:

$$RMSFE_v = \frac{1}{N} \sum_{i=1}^N \sqrt{\frac{1}{P} \sum_{t=T-P+1}^T \hat{e}_{v,i,t}^2}, \quad (9)$$

where $\hat{e}_{v,i,t}^2$ is the prediction error of a model on nowcast date v for state i and year t , T is the last year in the sample and P is the number of out-of-sample predictions.

For the density forecasts of per-capita CO2 emissions growth, we consider the Quantile Score (QS), which is a common metric used to evaluate a particular quantile forecast (see [Gneiting and Raftery, 2007](#); [Giacomini and Komunjer, 2005](#)), defined as follows,

$$QS_{v,\tau} = \frac{1}{N} \sum_{i=1}^N \frac{1}{P} \sum_{t=T-P+1}^T (\hat{Q}_{e_{v,i,t}}(\tau|X) - e_{v,i,t})(1(\hat{Q}_{e_{v,i,t}}(\tau|X) < e_{v,i,t}) - \tau), \quad (10)$$

where $1(\hat{Q}_{e_{v,i,t}}(\tau|X) < e_{v,i,t})$ is the indicator function that takes a value of 1 if the outcome is below the nowcast of the conditional quantile $\hat{Q}_{e_{v,i,t}}(\tau|X)$ and 0 otherwise. Then, when the quantile scores are aggregated, we define a discrete version of the Continuous Ranked Probability Score (CRPS) ([Gneiting and Ranjan, 2011](#)), as follows,

$$CRPS_v = \frac{1}{J} \sum_{j=1}^J \omega(\tau_j) QS(v, \tau_j), \quad (11)$$

where $J = 3$, $\tau_1 = 0.25$, $\tau_2 = 0.50$, $\tau_3 = 0.75$, and the weights $\omega(\tau_j)$ are set to 1 to account for equal weights across quantiles. As [Gneiting and Ranjan \(2011\)](#) point out, the discrete version of the CRPS constitutes a proper scoring rule that emerges as a particular instance of the continuous version. Furthermore, we examine the distribution of the aforementioned accuracy measures for each calendar, without averaging over the states. However, as [Fosten and Nandi \(2023b\)](#) observed, these results are merely indicative, as they are calculated with a small sample size.

Table 2: Weekly calendar of information availability (example for 2021)

	Calendar date		Latest information available for:				
	Weekly calendar (<i>v</i>)		CO2	EC	PI	ELEC	WECI
Backcast	1	2021:W1	2017	2018	2020:Q3	2020:M11	2020:W49
	2	2021:W2	2017	2018	2020:Q3	2020:M11	2020:W50
	3	2021:W3	2017	2018	2020:Q3	2020:M11	2020:W51
	4	2021:W4	2017	2018	2020:Q3	2020:M11	2020:W52
Nowcast	5	2021:W5	2017	2018	2020:Q3	2020:M12	2021:W1
	6	2021:W6	2017	2018	2020:Q3	2020:M12	2021:W2
	7	2021:W7	2017	2018	2020:Q3	2020:M12	2021:W3
	8	2021:W8	2017	2018	2020:Q3	2020:M12	2021:W4
	9	2021:W9	2018	2018	2020:Q4	2021:M1	2021:W5
	10	2021:W10	2018	2018	2020:Q4	2021:M1	2021:W6
	11	2021:W11	2018	2018	2020:Q4	2021:M1	2021:W7
	12	2021:W12	2018	2018	2020:Q4	2021:M1	2021:W8
	13	2021:W13	2018	2018	2020:Q4	2021:M2	2021:W9
	14	2021:W14	2018	2018	2020:Q4	2021:M2	2021:W10
	15	2021:W15	2018	2018	2020:Q4	2021:M2	2021:W11
	16	2021:W16	2018	2018	2020:Q4	2021:M2	2021:W12
	17	2021:W17	2018	2018	2020:Q4	2021:M3	2021:W13
	18	2021:W18	2018	2018	2020:Q4	2021:M3	2021:W14
	19	2021:W19	2018	2018	2020:Q4	2021:M3	2021:W15
	20	2021:W20	2018	2018	2020:Q4	2021:M3	2021:W16
	21	2021:W21	2018	2019	2021:Q1	2021:M4	2021:W17
	22	2021:W22	2018	2019	2021:Q1	2021:M4	2021:W18
	23	2021:W23	2018	2019	2021:Q1	2021:M4	2021:W19
	24	2021:W24	2018	2019	2021:Q1	2021:M4	2021:W20
	25	2021:W25	2018	2019	2021:Q1	2021:M5	2021:W21
	26	2021:W26	2018	2019	2021:Q1	2021:M5	2021:W22
	27	2021:W27	2018	2019	2021:Q1	2021:M5	2021:W23
	28	2021:W28	2018	2019	2021:Q1	2021:M5	2021:W24
	29	2021:W29	2018	2019	2021:Q1	2021:M6	2021:W25
	30	2021:W30	2018	2019	2021:Q1	2021:M6	2021:W26
	31	2021:W31	2018	2019	2021:Q1	2021:M6	2021:W27
	32	2021:W32	2018	2019	2021:Q1	2021:M6	2021:W28
	33	2021:W33	2018	2019	2021:Q2	2021:M7	2021:W29
	34	2021:W34	2018	2019	2021:Q2	2021:M7	2021:W30
	35	2021:W35	2018	2019	2021:Q2	2021:M7	2021:W31
	36	2021:W36	2018	2019	2021:Q2	2021:M7	2021:W32
	37	2021:W37	2018	2019	2021:Q2	2021:M8	2021:W33
	38	2021:W38	2018	2019	2021:Q2	2021:M8	2021:W34
	39	2021:W39	2018	2019	2021:Q2	2021:M8	2021:W35
	40	2021:W40	2018	2019	2021:Q2	2021:M8	2021:W36
	41	2021:W41	2018	2019	2021:Q2	2021:M9	2021:W37
	42	2021:W42	2018	2019	2021:Q2	2021:M9	2021:W38
	43	2021:W43	2018	2019	2021:Q2	2021:M9	2021:W39
	44	2021:W44	2018	2019	2021:Q2	2021:M9	2021:W40
	45	2021:W45	2018	2019	2021:Q3	2021:M10	2021:W41
	46	2021:W46	2018	2019	2021:Q3	2021:M10	2021:W42
	47	2021:W47	2018	2019	2021:Q3	2021:M10	2021:W43
	48	2021:W48	2018	2019	2021:Q3	2021:M10	2021:W44

Notes: This calendar is based on *Fosten and Nandi (2023b)*, and extended to accommodate weekly information of the WECI.

4 Nowcasting Results

This section presents the results of the pseudo-out-of-sample exercise described in the previous subsection. We report the results for the growth rate of per-capita EC and CO₂ emissions. In Appendix A.1, we present the figures for the original growth rates of energy consumption and CO₂ emissions, where similar results are documented.

4.1 Nowcasting energy consumption growth using panel MIDAS

We begin our discussion with the results from the panel MIDAS model used to nowcast the per-capita EC growth rate. Figure 2 plots the average RMSFE across states at various nowcast release points and for the different proposed models. RMSFE values are normalized by that of the historic unconditional mean benchmark model, with values below 1 indicating superior predictive accuracy. Our results indicate that, on average, incorporating quarterly, monthly, and/or weekly predictors is useful to better nowcast state-level energy consumption growth. We also observe that the RMSFE typically decreases as additional information is incorporated into the models, thus supporting the nowcast monotonicity evidenced in other studies (see, [Giannone et al., 2008](#); [Fosten and Nandi, 2023b](#)). For all competing models, the relative RMSFE is below 1.

Monthly electricity sales stands out as the most significant individual predictor for energy consumption growth. When analyzing the predictive performance of each model using only one predictor at a time, we observe that the RMSFE for the AR-M model consistently falls below that of the AR-Q and AR-W models. At the beginning of the third month of the calendar, when the first data on current-year electricity sales are released, the AR-M model shows a 20% improvement in predictive accuracy relative to the historical benchmark. Throughout the year, as additional data become available and are incorporated into the information set, the nowcast accuracy of the AR-M model further improves, reaching a peak of approximately 35% gains with respect to the benchmark.

Combining predictors with different sampling frequencies is beneficial for nowcasting in this application. Overall, models that include both the WECI and the monthly electricity sales simultaneously exhibit the best predictive performance. At all weeks of the calendar, the AR-W-M-Q model reports the smallest RMSFE, surpassing the AR-M model. The disparity between these two models increases over the year as more quarterly and weekly data are incorporated. By year-end, the difference in performance peaks at approximately 10%.

There is substantial variation in the performance of the nowcasting exercise across states. Table 3 detail the quantiles of the RMSFE distribution for the AR-W-M-Q model. Similar Tables for the other models are presented in Appendix A.2. As observed, almost all quantiles of the relative RMSFE fall below 1, demonstrating improvements over the benchmark model in nearly every state. In some states at the left tail of the distribution, the improvement exceeds 60%. Additionally, a consistent decrease in all quantiles is observed as more information becomes available throughout the year.

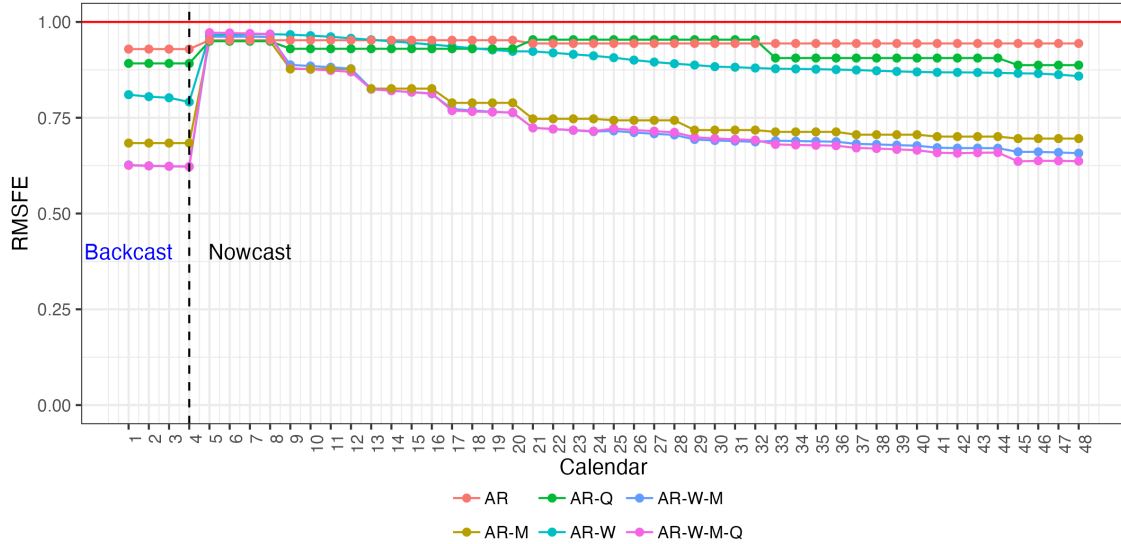
Table 3: Distribution of relative RMSFE across states for AR-W-M-Q model

Calendar (<i>v</i>)		10%	25%	50%	75%	90%	RMSE
Backcast	2021:W1	0.379	0.456	0.605	0.759	0.955	0.626
	2021:W2	0.369	0.452	0.595	0.758	0.950	0.624
	2021:W3	0.370	0.452	0.588	0.757	0.945	0.623
	2021:W4	0.378	0.452	0.584	0.750	0.938	0.623
Nowcast	2021:W5	0.848	0.904	0.965	1.042	1.157	0.972
	2021:W6	0.849	0.904	0.969	1.044	1.152	0.971
	2021:W7	0.845	0.901	0.971	1.047	1.145	0.970
	2021:W8	0.842	0.900	0.971	1.050	1.139	0.968
	2021:W9	0.724	0.790	0.880	0.962	1.057	0.879
	2021:W10	0.716	0.787	0.877	0.960	1.055	0.876
	2021:W11	0.708	0.787	0.873	0.960	1.053	0.873
	2021:W12	0.699	0.785	0.870	0.959	1.050	0.870
	2021:W13	0.637	0.696	0.848	0.930	1.030	0.824
	2021:W14	0.638	0.691	0.838	0.932	1.023	0.821
	2021:W15	0.638	0.687	0.827	0.935	1.018	0.817
	2021:W16	0.630	0.684	0.819	0.929	1.012	0.814
	2021:W17	0.562	0.691	0.760	0.892	0.986	0.769
	2021:W18	0.561	0.689	0.758	0.891	0.989	0.766
	2021:W19	0.560	0.687	0.757	0.891	0.990	0.765
	2021:W20	0.561	0.685	0.757	0.890	0.987	0.764
	2021:W21	0.512	0.620	0.739	0.859	0.940	0.723
	2021:W22	0.505	0.617	0.734	0.862	0.941	0.721
	2021:W23	0.505	0.613	0.729	0.855	0.941	0.718
	2021:W24	0.502	0.609	0.717	0.854	0.945	0.715
	2021:W25	0.528	0.624	0.734	0.838	0.935	0.722
	2021:W26	0.525	0.622	0.725	0.838	0.941	0.718
	2021:W27	0.519	0.620	0.718	0.840	0.939	0.715
	2021:W28	0.513	0.616	0.709	0.842	0.946	0.712
	2021:W29	0.490	0.585	0.716	0.816	0.975	0.699
	2021:W30	0.482	0.583	0.708	0.813	0.981	0.696
	2021:W31	0.475	0.581	0.704	0.808	0.982	0.694
	2021:W32	0.480	0.574	0.702	0.805	0.989	0.692
	2021:W33	0.493	0.549	0.688	0.828	0.947	0.680
	2021:W34	0.493	0.548	0.687	0.826	0.948	0.679
	2021:W35	0.490	0.551	0.681	0.821	0.948	0.678
	2021:W36	0.487	0.553	0.675	0.817	0.949	0.677
	2021:W37	0.465	0.543	0.673	0.798	0.967	0.671
	2021:W38	0.464	0.541	0.669	0.793	0.963	0.670
	2021:W39	0.467	0.538	0.663	0.795	0.975	0.667
	2021:W40	0.466	0.533	0.659	0.797	0.977	0.665
	2021:W41	0.413	0.522	0.660	0.827	0.966	0.659
	2021:W42	0.409	0.519	0.659	0.825	0.961	0.658
	2021:W43	0.408	0.520	0.659	0.822	0.958	0.659
	2021:W44	0.408	0.519	0.659	0.819	0.970	0.659
	2021:W45	0.384	0.491	0.615	0.804	1.014	0.636
	2021:W46	0.382	0.491	0.620	0.806	1.023	0.638
	2021:W47	0.382	0.486	0.620	0.806	1.026	0.637
	2021:W48	0.383	0.483	0.619	0.806	1.031	0.637

Note: The dependent variable is the state-level energy consumption per capita growth. RMSFE relative to a historical mean benchmark.

This exercise demonstrates that the use of timely information is valuable for a better nowcasting of state-level energy consumption. Compared to the study by [Fosten and Nandi \(2023b\)](#), our analysis reveals better nowcasting accuracy, possibly due to recent data revisions and the strategic combination of indicators sampled at different frequencies.

Figure 2: RMSFE across states for EC per capita growth



Notes: The AR-W-M-Q model incorporates an autoregressive (AR) component, the weekly economic condition index (W), the monthly electricity sales (M), and the quarterly PI data (Q). The benchmark model is a historic mean for electricity consumption growth. The benchmark normalizes the RMSFE figures at the first release date. Consequently, any points below 1 indicate that the RMSFE is lower than that of the benchmark.

4.2 Density nowcast of CO2 emissions growth using a bridge equation

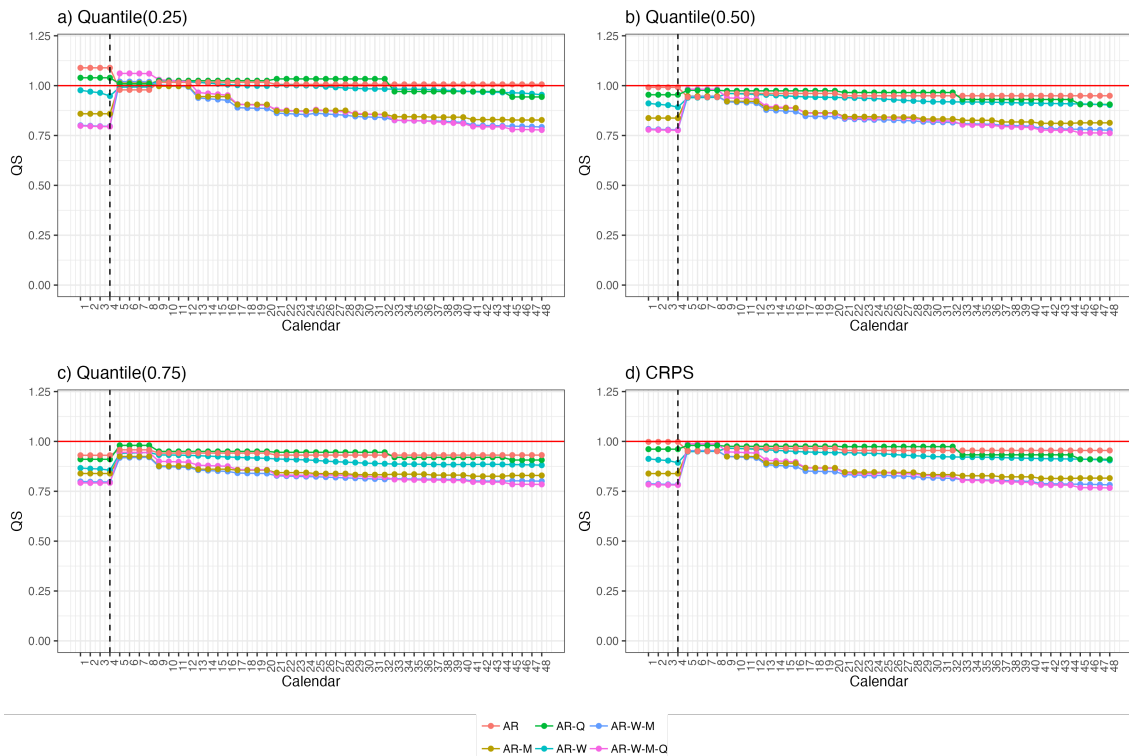
Using the timely predictions of per-capita energy consumption growth for the target year, we now generate density nowcasts of per-capita CO2 emissions growth through a bridge equation. The quantile levels, set at $\tau_1 = 0.25$, $\tau_2 = 0.50$, $\tau_3 = 0.75$, are chosen to capture predictions for the central part and the tails of the distribution. These density nowcasts are compared to the historical quantile benchmark for each week of the calendar year.

Figure 3 presents quantile scores and the CRPS measuring the predictive accuracy of each proposed model throughout the calendar year. In all models and weeks, the CRPS values are below 1, indicating that our density quantile approach provides an improvement over the benchmark. The gains in predictive accuracy observed in energy consumption growth are translated into the nowcasting of CO2 emissions. The best-performing models are AR-M, AR-W-M, and AR-W-M-Q, with the latter showing marginally superior performance due to the simultaneous inclusion of all predictors. Moreover, notice that between weeks 4 and 12, when limited information on current-year predictors is available, the CRSP are close to 1. As more data becomes available throughout the year, the precision of the nowcasts increases monotonically until reaching a maximum gain of around

25% at the end of the year in our best model. Nowcasts show better performance at the median and the 0.75 quantile, while they are less effective at the 0.25 quantile, particularly in the early part of the calendar year. As more information is incorporated, the gains in predictive accuracy become similar across the distribution.

Table 4 complements our analysis by presenting the distribution of relative CRPS across states for the AR-W-M-Q model. Appendix A.3 provides detailed tables reporting the distribution of the QS for each individual quantile level. Results indicate significant improvements in predictive accuracy over the historical quantile benchmark across nearly all states and quantile levels.

Figure 3: Quantile accuracy measures for CO2 per capita growth



Notes: CO2 per capita growth nowcasts based on the AR-W-M-Q model for EC growth, which incorporates an autoregressive (AR) component, the weekly economic condition index (W), the monthly electricity sales (M), and the quarterly PI data (Q). The benchmark model is a historic mean for CO2 per capita growth. The benchmark normalizes the figures at the first release date. Consequently, any points below 1 indicate that the respective accuracy measures is lower than that of the benchmark.

4.3 Direct density nowcast of CO2 emissions growth

This subsection evaluates the nowcasts from the best-performing model that utilizes a bridge equation against those derived from a model that applies direct panel quantile regression to CO2 emissions growth data, without relying on predictions of energy consumption growth. Figure 4 presents a comparative analysis of the quantile scores and the CRPS between the AR-W-M-Q model and the direct approach. Both methods show similar

Table 4: Distribution of relative CRSP across states for AR-W-M-Q model

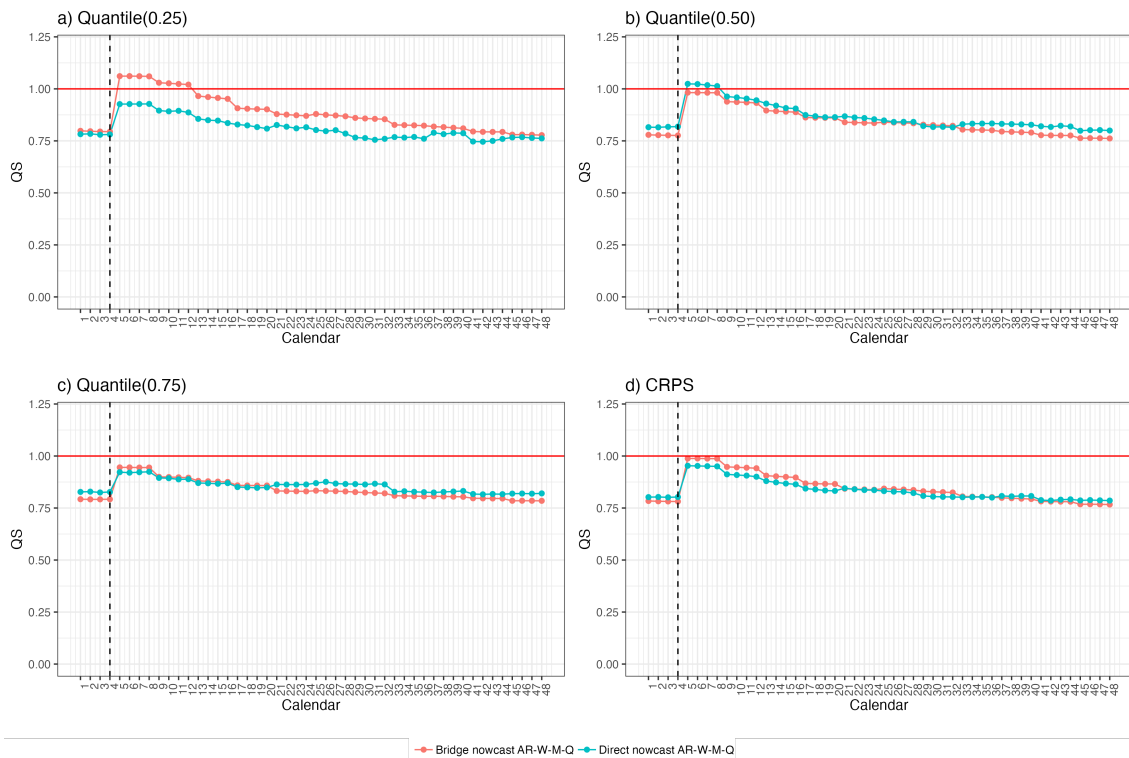
Calendar (v)		10%	25%	50%	75%	90%	CRSP
Backcast	2021:W1	0.628	0.662	0.754	0.870	0.966	0.779
	2021:W2	0.625	0.659	0.756	0.868	0.963	0.778
	2021:W3	0.621	0.660	0.756	0.868	0.962	0.777
	2021:W4	0.620	0.663	0.756	0.868	0.960	0.776
Nowcast	2021:W5	0.785	0.874	0.988	1.051	1.189	0.982
	2021:W6	0.783	0.876	0.986	1.052	1.189	0.982
	2021:W7	0.781	0.876	0.983	1.053	1.188	0.982
	2021:W8	0.778	0.878	0.982	1.054	1.186	0.981
	2021:W9	0.727	0.855	0.939	1.008	1.143	0.939
	2021:W10	0.723	0.856	0.938	1.001	1.144	0.937
	2021:W11	0.717	0.856	0.936	0.996	1.145	0.935
	2021:W12	0.714	0.852	0.933	0.994	1.144	0.933
	2021:W13	0.705	0.833	0.893	0.967	1.071	0.896
	2021:W14	0.702	0.831	0.887	0.964	1.071	0.893
	2021:W15	0.698	0.831	0.883	0.963	1.070	0.890
	2021:W16	0.693	0.832	0.878	0.962	1.069	0.888
	2021:W17	0.684	0.770	0.840	0.958	1.043	0.862
	2021:W18	0.681	0.772	0.841	0.957	1.045	0.861
	2021:W19	0.680	0.776	0.840	0.955	1.047	0.861
	2021:W20	0.680	0.777	0.839	0.958	1.050	0.861
	2021:W21	0.676	0.731	0.834	0.930	1.015	0.840
	2021:W22	0.669	0.730	0.836	0.927	1.016	0.838
	2021:W23	0.664	0.731	0.834	0.924	1.009	0.837
	2021:W24	0.661	0.727	0.831	0.924	1.016	0.836
	2021:W25	0.667	0.728	0.832	0.928	1.018	0.840
	2021:W26	0.663	0.725	0.829	0.928	1.018	0.838
	2021:W27	0.659	0.717	0.830	0.925	1.019	0.836
	2021:W28	0.656	0.710	0.829	0.919	1.018	0.835
	2021:W29	0.652	0.723	0.790	0.923	1.020	0.828
	2021:W30	0.650	0.718	0.786	0.920	1.026	0.826
	2021:W31	0.648	0.716	0.780	0.918	1.034	0.824
	2021:W32	0.645	0.714	0.776	0.913	1.039	0.823
	2021:W33	0.606	0.675	0.773	0.908	1.023	0.804
	2021:W34	0.612	0.678	0.770	0.905	1.024	0.803
	2021:W35	0.619	0.677	0.766	0.901	1.024	0.802
	2021:W36	0.621	0.674	0.765	0.896	1.024	0.801
	2021:W37	0.613	0.671	0.776	0.859	1.011	0.795
	2021:W38	0.610	0.664	0.776	0.856	1.013	0.793
	2021:W39	0.607	0.661	0.777	0.856	1.014	0.792
	2021:W40	0.605	0.662	0.776	0.857	1.016	0.790
	2021:W41	0.597	0.670	0.769	0.851	1.005	0.777
	2021:W42	0.595	0.672	0.767	0.849	1.002	0.776
	2021:W43	0.595	0.668	0.767	0.846	1.003	0.776
	2021:W44	0.595	0.667	0.766	0.843	1.002	0.776
	2021:W45	0.567	0.663	0.751	0.812	0.972	0.763
	2021:W46	0.568	0.660	0.749	0.812	0.973	0.763
	2021:W47	0.567	0.657	0.747	0.812	0.973	0.763
	2021:W48	0.566	0.653	0.746	0.811	0.972	0.762

Note: The dependent variable is the state-level per-capita CO2 emissions growth.

performance in terms of CRPS, with the best-case scenario indicating an approximate 25% improvement relative to the historical unconditional benchmark. However, at the beginning of the calendar year, the direct method demonstrates slightly superior performance. The enhanced early-year performance of the direct approach is attributed to its better accuracy in nowcasting at the 0.25 quantile level. This advantage persists throughout the year, suggesting that the direct method may be more effective in capturing lower tail dynamics in the distribution of CO2 emissions growth.

The observed difference in performance between the direct method and the AR-W-M-Q model can be attributed to the prediction errors inherent in the bridge equation employed by the latter. These errors likely influence the overall accuracy of the AR-W-M-Q model, particularly affecting its efficiency in early-year predictions and at lower quantile levels. Despite these challenges, a valid argument for continuing to use a bridge equation lies in its capacity to generate timely predictions of energy consumption growth, object of specific interest to policymakers and researchers.

Figure 4: Direct vs bridge approaches



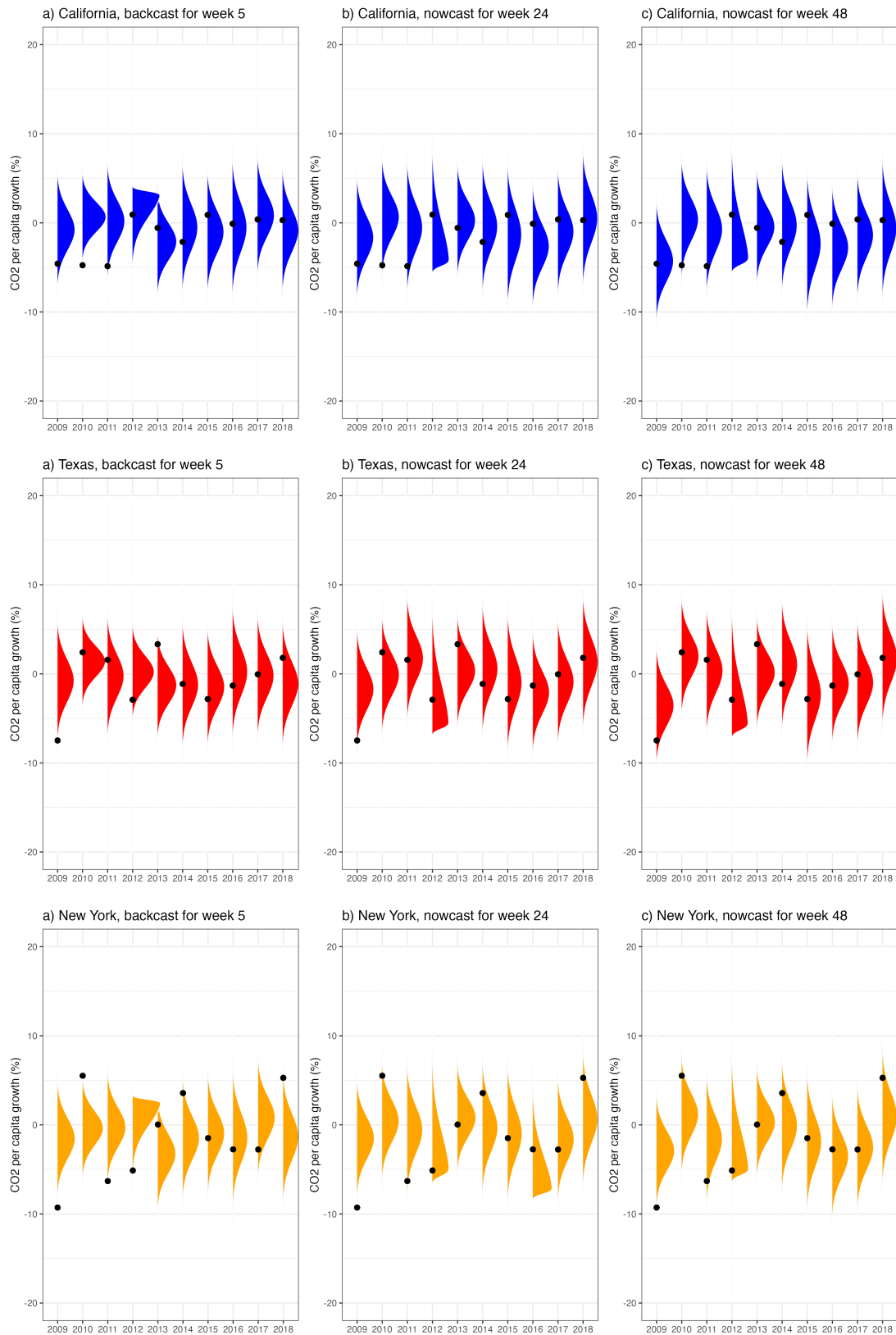
Notes: CO2 per capita growth nowcasts based on the AR-W-M-Q model for EC growth, which incorporates an autoregressive (AR) component, the weekly economic condition index (W), the monthly electricity sales (M), and the quarterly PI data (Q). The direct model incorporates the W-M-Q component instead of EC per capita growth predictions, and the common correlated effect of CO2 per capita growth. The benchmark model is a historic mean for CO2 per capita growth. The benchmark normalizes the figures at the first release date. Consequently, any points below 1 indicate that the respective accuracy measures is lower than that of the benchmark.

4.4 High-frequency density nowcasts for selected states

This section illustrates the behavior of our timely quantile predictions of per-capita CO₂ emissions growth throughout the calendar year. Figure 5 displays the predicted densities for weeks 5, 24, and 48, and compare these predictions with the realized values of the target variable. Following [Adrian et al. \(2019\)](#), full continuous conditional densities are constructed by fitting a generalized skewed Student's distribution to the discrete conditional quantiles predicted at each nowcasting point. Specific weeks are chosen to examine how predictions for the current year improve as more information becomes available over the calendar. Results are presented for the AR-W-M-Q model and focus on California, Texas, and New York, states that annually report the highest CO₂ emissions records.

Our analysis indicates that in most cases, the actual values of CO₂ emissions growth (represented by black dots) fall within the range of the predicted densities. Improvements in predictive accuracy across the calendar are evident, particularly if we compare density predictions in week 5 versus week 24. As additional data become available, the median of the predicted density moves closer to the actual observed value, providing a visual confirmation of the decreasing CRPS highlighted earlier in this paper. The performance of our approach exhibits considerable variability across different states and years. For Texas and New York, the model demonstrates relatively strong predictive accuracy between 2014 and 2017. In contrast, for California, the model achieves better results between 2013 and 2015.

Figure 5: Density nowcast for per-capita CO₂ emissions for California, Texas, and New York

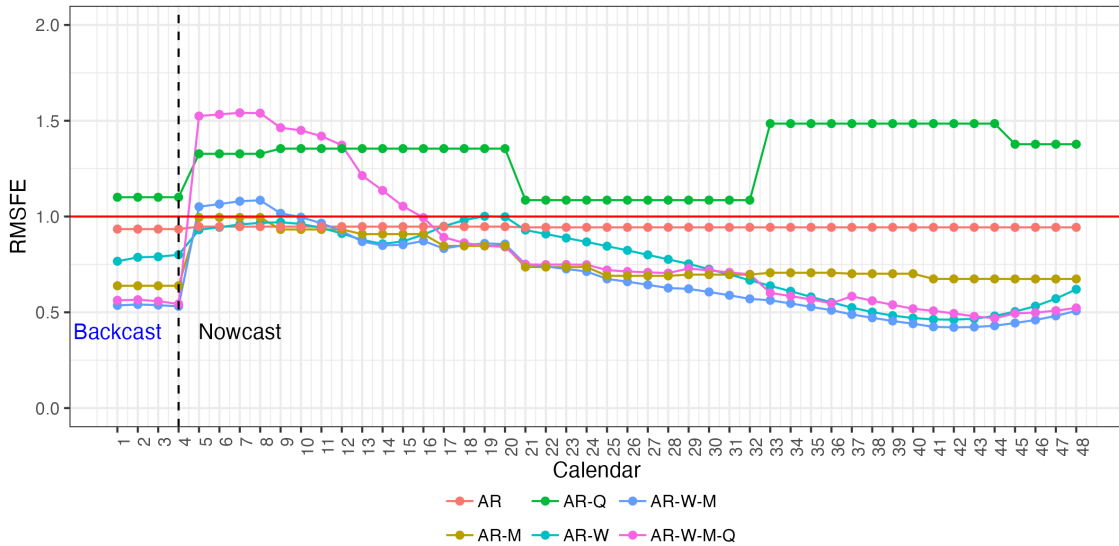


Notes: Black dots are the realized value of CO₂ per capita growth. The densities are obtained from the quantile predictions obtained through the AR-W-M-Q model using a bridge equation.

4.5 Nowcasting during the COVID 19 period

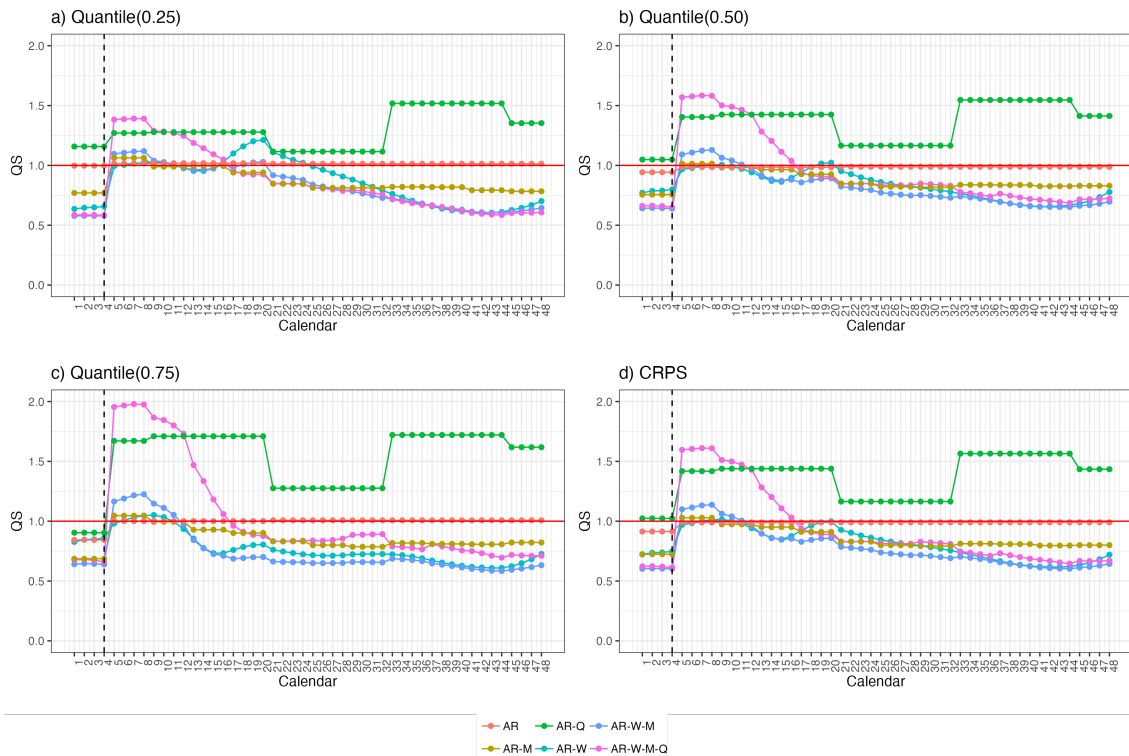
We evaluate how effectively the various nowcasting approaches capture the abrupt decline in CO2 emissions during the COVID-19 period and the subsequent recovery. To this end, we extend our out-of-sample analysis to include the years 2019 through 2021 and compute the accuracy measures reported in Figures 6 and 7. For both target variables, incorporating quarterly PI data significantly worsens the predictions compared to the historical benchmark. In contrast, including monthly and weekly predictors yields substantial improvements, specially after week 15. The models that include the WECI achieve the lowest RMSFE and CRPS, with gains surpassing those observed in non-COVID periods. Figure 8 presents the densities constructed from the quantile predictions generated by the AR-W-M model via a bridge equation, illustrating how effectively the model nowcasts CO2 emissions across selected states as more information becomes available throughout the year. By week 48, the predicted densities are closer to the observed values.

Figure 6: COVID-19: RMSFE across states for EC per capita growth



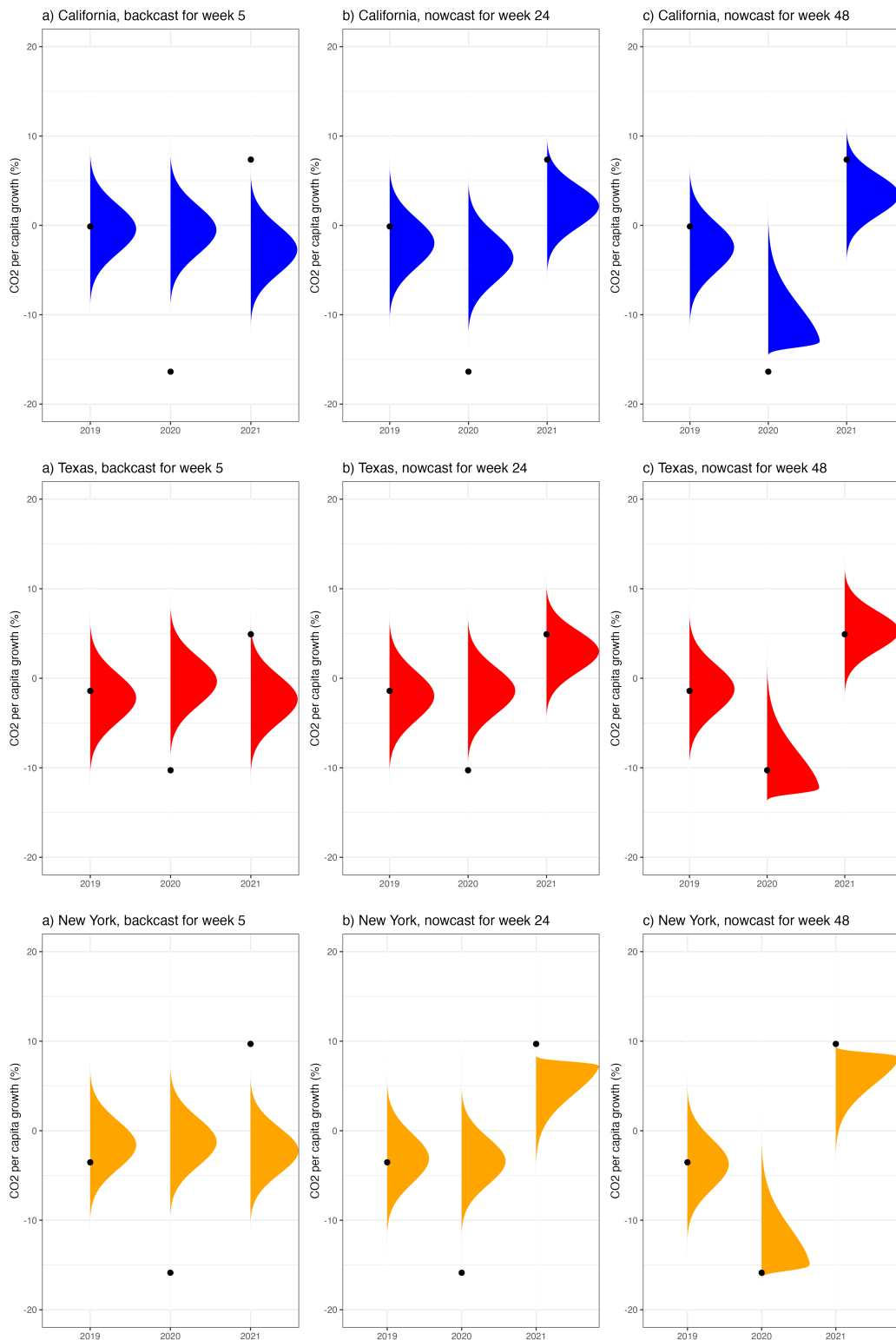
Notes: The AR-W-M-Q model incorporates an autoregressive (AR) component, the weekly economic condition index (W), the monthly electricity sales (M), and the quarterly PI data (Q). The benchmark model is a historic mean for electricity consumption growth. The benchmark normalizes the RMSFE figures at the first release date. Consequently, any points below 1 indicate that the RMSFE is lower than that of the benchmark.

Figure 7: COVID-19: Quantile accuracy measures for CO2 per capita growth



Notes: CO2 per capita growth nowcasts based on the AR-W-M-Q model for EC growth, which incorporates an autoregressive (AR) component, the weekly economic condition index (W), the monthly electricity sales (M), and the quarterly PI data (Q). The benchmark model is a historic mean for CO2 per capita growth. The benchmark normalizes the figures at the first release date. Consequently, any points below 1 indicate that the respective accuracy measures is lower than that of the benchmark.

Figure 8: COVID-19: Density nowcast for per-capita CO₂ emissions for California, Texas, and New York



Notes: Black dots are the realized value of CO₂ per capita growth. The densities are obtained from the quantile predictions obtained through the AR-W-M model using a bridge equation.

5 Conclusions

In this paper, we introduced a panel nowcasting methodology to obtain high-frequency nowcasts of state-level per-capita energy consumption and CO₂ emissions growth in the U.S. Our methodology extends the approach of [Fosten and Nandi \(2023b\)](#) by incorporating the state-level weekly economic conditions index of [Baumeister et al. \(2024\)](#), and by utilizing panel quantile regressions to produce density nowcasts of per-capita CO₂ emissions growth. This enhancement enables us to report not only the expected trajectory of per-capita CO₂ emissions growth but also the uncertainty surrounding this central path. In our out-of-sample exercise, covering the period from 2009 to 2018, we found that the model incorporating economic predictors at mixed frequencies consistently outperformed other models. Specifically, the most effective model includes data at weekly, monthly, and quarterly intervals, and applies a restricted Almon lag polynomial to approximate the high-frequency weekly component. The inclusion of weekly data is particularly useful to better nowcast during the COVID-19 period.

The application of our nowcasting methodology to the domains of energy consumption and CO₂ emissions is highly pertinent, particularly due to the significant delays in the publication of official data. The publication delay for CO₂ emissions data extends to approximately two years and three months after the end of the reference year, while the delay for energy consumption data is around 18 months. Our methodology leverages the more prompt availability of economic data to provide early insights to policymakers on the evolution of critical environmental variables. As the year progresses and more data becomes available, the accuracy of our predictions improves. This approach enables a timely and precise tracking of anthropogenic CO₂ emissions at both national and sub-national levels, which is crucial for the development of effective climate policies and for meeting long-term international commitments to combat climate change.

References

- Adrian, T., N. Boyarchenko, and D. Giannone (2019, 9). Vulnerable Growth. *American Economic Review* 109, 1263–1289.
- AR6-IPCC (2021). *Climate Change 2021: The Physical Science Basis*. [Masson-Delmotte V, Zhai P, Pirani A et al. (eds)]. Cambridge and New York: Cambridge University Press.
- Auffhammer, M. and R. Steinhauser (2012). Forecasting The Path of U.S. CO2 Emissions Using State-Level Information. *The Review of Economics and Statistics* 94(1), 172–185.
- Azomahou, T., F. Laisney, and P. N. Van (2006). Economic Development and CO2 Emissions: A Nonparametric Panel Approach. *Journal of Public Economics* 90(6), 1347–1363.
- Azzalini, A. and A. Capitanio (2003, 9). Distributions Generated by Perturbation of Symmetry with Emphasis on a Multivariate Skew t-distribution. *Journal of the Royal Statistical Society. Series B: Statistical Methodology* 65, 367–389.
- Baumeister, C., D. Leiva-León, and E. Sims (2024). Tracking Weekly State-Level Economic Conditions. *The Review of Economics and Statistics* 106(2), 483–504.
- Bañbura, M., D. Giannone, M. Modugno, and L. Reichlin (2013, 9). Now-casting and the real-time data flow. *Handbook of Economic Forecasting* 2, 195–237.
- Bennedsen, M., E. Hillebrand, and S. Jensen (2023). A Neural Network Approach to the Environmental Kuznets Curve. *Energy Economics* 126, 106985.
- Bennedsen, M., E. Hillebrand, and S. J. Koopman (2021). Modeling, Forecasting, and Nowcasting U.S. CO2 Emissions Using Many Macroeconomic Predictors. *Energy Economics* 96, 105–118.
- Carriero, A., T. E. Clark, and M. Marcellino (2022, 9). Nowcasting tail risk to economic activity at a weekly frequency. *Journal of Applied Econometrics* 37, 843–866.
- Chuliá, H., I. Garrón, and J. M. Uribe (2024, 4). Daily growth at risk: Financial or real drivers? the answer is not always the same. *International Journal of Forecasting* 40, 762–776.
- Dong, Y., K. C. Armour, C. Proistosescu, T. Andrews, D. S. Battisti, P. M. Forster, D. Paynter, C. J. Smith, and H. Shiogama (2021). Biased Estimates of Equilibrium Climate Sensitivity and Transient Climate Response Derived From Historical CMIP6 Simulations. *Geophysical Research Letters* 48(24), e2021GL095778.
- Ferrara, L., M. Mogliani, and J.-G. Sahuc (2022). High-frequency Monitoring of Growth at Risk. *International Journal of Forecasting* 38(2), 582–595.
- Froni, C., M. Marcellino, and C. Schumacher (2015, 1). Unrestricted mixed data sampling (midas): Midas regressions with unrestricted lag polynomials. *Journal of the Royal Statistical Society Series A: Statistics in Society* 178, 57–82.
- Fosten, J. and S. Nandi (2023a, 9). Nowcasting from cross-sectionally dependent panels. *Journal of Applied Econometrics* 38, 898–919.
- Fosten, J. and S. Nandi (2023b). Nowcasting U.S. State-level CO2 Emissions and Energy Consumption. *International Journal of Forecasting*.
- Friedlingstein, P., M. O’Sullivan, M. W. Jones, R. M. Andrew, D. C. E. Bakker, J. Hauck, P. Landschützer, C. Le Quéré, I. T. Lujckx, G. P. Peters, W. Peters, J. Pongratz, C. Schwingshackl, S. Sitch, J. G. Canadell, P. Ciais, R. B. Jackson, S. R. Alin, P. Anthoni, L. Barbero, N. R. Bates, M. Becker, N. Bellouin, B. Decharme, L. Bopp, I. B. M. Brasika, P. Cadule, M. A. Chamberlain, N. Chandra, T.-T.-T. Chau, F. Chevallier, L. P. Chini, M. Cronin, X. Dou, K. Enyo, W. Evans, S. Falk, R. A. Feely, L. Feng, D. J. Ford, T. Gasser, J. Ghattas,

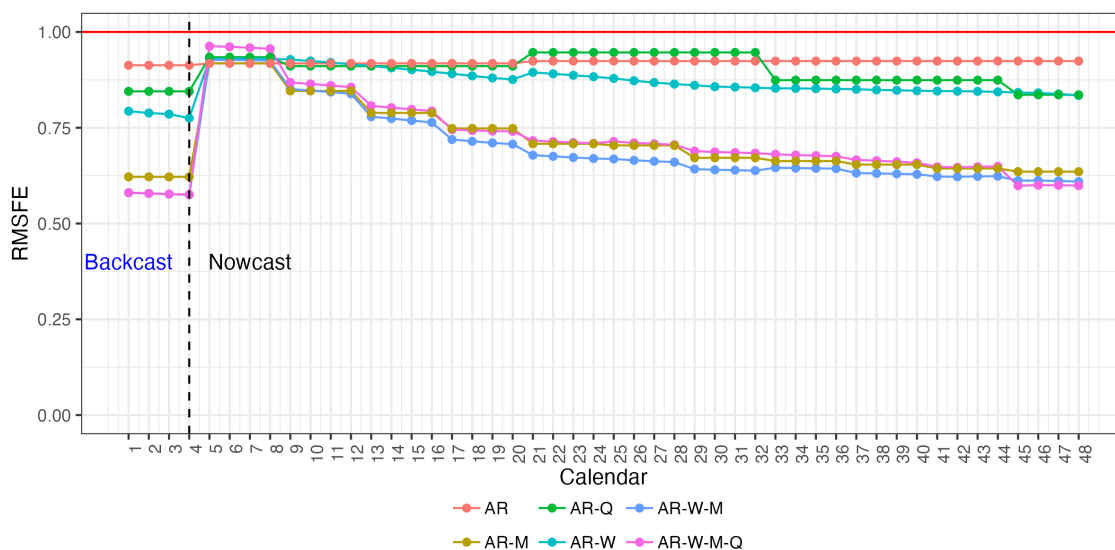
- T. Gkritzalis, G. Grassi, L. Gregor, N. Gruber, O. Gürses, I. Harris, M. Hefner, J. Heinke, R. A. Houghton, G. C. Hurtt, Y. Iida, T. Ilyina, A. R. Jacobson, A. Jain, T. Jarníková, A. Jersild, F. Jiang, Z. Jin, F. Joos, E. Kato, R. F. Keeling, D. Kennedy, K. Klein Goldewijk, J. Knauer, J. I. Korsbakken, A. Körtzinger, X. Lan, N. Lefèvre, H. Li, J. Liu, Z. Liu, L. Ma, G. Marland, N. Mayot, P. C. McGuire, G. A. McKinley, G. Meyer, E. J. Morgan, D. R. Munro, S.-I. Nakaoka, Y. Niwa, K. M. O'Brien, A. Olsen, A. M. Omar, T. Ono, M. Paulsen, D. Pierrot, K. Pockock, B. Poulter, C. M. Powis, G. Rehder, L. Resplandy, E. Robertson, C. Rödenbeck, T. M. Rosan, J. Schwinger, R. Séférian, T. L. Smallman, S. M. Smith, R. Sospedra-Alfonso, Q. Sun, A. J. Sutton, C. Sweeney, S. Takao, P. P. Tans, H. Tian, B. Tilbrook, H. Tsujino, F. Tubiello, G. R. van der Werf, E. van Ooijen, R. Wanninkhof, M. Watanabe, C. Wimart-Rousseau, D. Yang, X. Yang, W. Yuan, X. Yue, S. Zaehle, J. Zeng, and B. Zheng (2023). Global Carbon Budget 2023. *Earth System Science Data* 15(12), 5301–5369.
- Ghysels, E., P. Santa-Clara, and R. Valkanov (2006). Predicting volatility: Getting the most out of return data sampled at different frequencies. In *Journal of Econometrics*, Volume 131.
- Giacomini, R. and I. Komunjer (2005). Evaluation and Combination of Conditional Quantile Forecasts. *Journal of Business & Economic Statistics* 23(4), 416–431.
- Giannone, D., L. Reichlin, and D. Small (2008, 9). Nowcasting: The real-time informational content of macroeconomic data. *Journal of Monetary Economics* 55, 665–676.
- Gneiting, T. and A. E. Raftery (2007). Strictly proper scoring rules, prediction, and estimation. *Journal of the American Statistical Association* 102, 359–378.
- Gneiting, T. and R. Ranjan (2011). Comparing density forecasts using threshold- and quantile-weighted scoring rules. *Journal of Business & Economic Statistics* 29, 411–422.
- Grossman, G. M. and A. B. Krueger (1991, November). Environmental Impacts of a North American Free Trade Agreement. Working Paper 3914, National Bureau of Economic Research.
- Jayachandran, S. (2022). How Economic Development Influences the Environment. *Annual Review of Economics* 14, 229–252.
- Jensen, S. (2021). *Use of Machine Learning in Climate Econometrics*. Phd thesis, Aarhus University.
- Jones, M. W., G. P. Peters, T. Gasser, R. M. Andrew, C. Schwingshackl, J. Gütschow, R. A. Houghton, P. Friedlingstein, J. Pongratz, and C. Le Quéré (2023). National Contributions to Climate Change Due to Historical Emissions of Carbon Dioxide, Methane, and Nitrous Oxide Since 1850. *Scientific Data* 10(1), 155.
- Koenker, R. (2004). Quantile regression for longitudinal data. *Journal of Multivariate Analysis* 91(1), 74–89.
- Magazzino, C., M. Gallegati, and F. Giri (2023). The Environmental Kuznets Curve in a long-term perspective: Parametric vs semi-parametric models. *Environmental Impact Assessment Review* 98, 106973.
- Mogliani, M. and A. Simoni (2021, 9). Bayesian midas penalized regressions: Estimation, selection, and prediction. *Journal of Econometrics* 222, 833–860.
- Smith, C. J., R. J. Kramer, G. Myhre, K. Alterskjær, W. Collins, A. Sima, O. Boucher, J.-L. Dufresne, P. Nabat, M. Michou, S. Yukimoto, J. Cole, D. Paynter, H. Shiogama, F. M. O'Connor, E. Robertson, A. Wiltshire, T. Andrews, C. Hannay, R. Miller, L. Nazarenko, A. Kirkevåg, D. Olivie, S. Fiedler, A. Lewinschal, C. Mackallah, M. Dix, R. Pincus, and P. M. Forster (2020). Effective Radiative Forcing and Adjustments in CMIP6 Models. *Atmospheric Chemistry and Physics* 20(16), 9591–9618.

A Appendix

A.1 Results of the nowcasting exercise of the growth rate of energy consumption

The baseline analysis of this document addresses the nowcasting of the **per-capita** growth rate of energy consumption and CO2 emissions. In this Appendix, we present the results using the original quantities of these variables without normalization by population. The findings for the growth rate of energy consumption align qualitatively with those of the baseline analysis. Specifically, models that incorporate both weekly and monthly indicators simultaneously exhibit the best predictive performance. Quantitatively, these models demonstrate even stronger gains in predictive accuracy compared to the per-capita analysis, achieving an average improvement of around 40% with respect to the historical mean benchmark by the end of the calendar year with the AR-W-M-Q model. These gains are translated to the nowcast of the growth rate of CO2 emissions. These results are omitted from this appendix due to space limitations but can be shared on request.

Figure A1: RMSFE across states for EC growth



Notes: The AR-W-M-Q model incorporates an autoregressive (AR) component, the weekly economic condition index (W), the monthly electricity sales (M), and the quarterly PI data (Q). The benchmark model is a historic mean for electricity consumption growth. The benchmark normalizes the RMSFE figures at the first release date. Consequently, any points below 1 indicate that the RMSFE is lower than that of the benchmark.

Table A1: Distribution of relative RMSFE across states for AR-W model

Calendar (v)		10%	25%	50%	75%	90%	RMSE
Backcast	2021:W1	0.624	0.705	0.790	0.874	0.955	0.793
	2021:W2	0.613	0.691	0.785	0.868	0.961	0.788
	2021:W3	0.612	0.682	0.771	0.866	0.955	0.786
	2021:W4	0.610	0.670	0.761	0.847	0.971	0.775
Nowcast	2021:W5	0.803	0.870	0.949	1.011	1.040	0.930
	2021:W6	0.804	0.874	0.951	1.009	1.042	0.930
	2021:W7	0.804	0.876	0.951	1.005	1.045	0.931
	2021:W8	0.802	0.877	0.955	1.006	1.047	0.930
	2021:W9	0.798	0.878	0.957	0.999	1.049	0.928
	2021:W10	0.793	0.876	0.959	0.991	1.044	0.924
	2021:W11	0.787	0.873	0.951	0.990	1.039	0.920
	2021:W12	0.781	0.870	0.943	0.990	1.034	0.916
	2021:W13	0.776	0.865	0.938	0.982	1.028	0.911
	2021:W14	0.770	0.857	0.934	0.975	1.021	0.906
	2021:W15	0.756	0.854	0.932	0.968	1.021	0.902
	2021:W16	0.740	0.845	0.932	0.964	1.018	0.896
	2021:W17	0.732	0.838	0.923	0.963	1.016	0.891
	2021:W18	0.735	0.830	0.912	0.957	1.008	0.885
	2021:W19	0.740	0.822	0.903	0.952	1.003	0.880
	2021:W20	0.739	0.816	0.901	0.946	0.998	0.876
	2021:W21	0.748	0.828	0.942	0.975	1.010	0.895
	2021:W22	0.737	0.825	0.939	0.977	1.009	0.891
	2021:W23	0.727	0.814	0.930	0.977	1.009	0.887
	2021:W24	0.718	0.811	0.918	0.974	1.007	0.883
	2021:W25	0.709	0.812	0.912	0.967	1.006	0.879
	2021:W26	0.701	0.810	0.898	0.960	1.009	0.873
	2021:W27	0.695	0.806	0.887	0.948	1.012	0.868
	2021:W28	0.690	0.806	0.878	0.941	1.016	0.864
	2021:W29	0.686	0.801	0.873	0.938	1.019	0.861
	2021:W30	0.681	0.797	0.867	0.936	1.018	0.857
	2021:W31	0.678	0.797	0.870	0.938	1.017	0.856
	2021:W32	0.677	0.794	0.869	0.939	1.015	0.854
	2021:W33	0.675	0.787	0.863	0.942	1.013	0.853
	2021:W34	0.676	0.783	0.862	0.943	1.011	0.853
	2021:W35	0.677	0.779	0.860	0.942	1.008	0.852
	2021:W36	0.679	0.775	0.858	0.939	1.007	0.851
	2021:W37	0.681	0.770	0.856	0.940	1.005	0.850
	2021:W38	0.682	0.766	0.854	0.944	1.003	0.849
	2021:W39	0.684	0.760	0.851	0.946	1.001	0.848
	2021:W40	0.686	0.755	0.848	0.948	0.999	0.847
	2021:W41	0.687	0.754	0.849	0.950	0.997	0.846
	2021:W42	0.689	0.755	0.851	0.952	0.995	0.845
	2021:W43	0.689	0.753	0.857	0.947	0.992	0.845
	2021:W44	0.688	0.749	0.859	0.944	0.993	0.844
	2021:W45	0.686	0.745	0.852	0.944	0.995	0.842
	2021:W46	0.684	0.743	0.845	0.947	0.996	0.841
	2021:W47	0.682	0.741	0.840	0.941	0.994	0.838
	2021:W48	0.678	0.740	0.836	0.933	0.990	0.834

Note: The dependent variable is the state-level EC growth.

Table A2: Distribution of relative RMSFE across states for AR-W-M model

Calendar (v)		10%	25%	50%	75%	90%	RMSE
Backcast	2021:W1	0.340	0.423	0.567	0.703	0.862	0.580
	2021:W2	0.340	0.416	0.565	0.698	0.868	0.578
	2021:W3	0.337	0.414	0.562	0.697	0.877	0.577
	2021:W4	0.337	0.414	0.558	0.695	0.885	0.575
Nowcast	2021:W5	0.784	0.899	0.938	1.005	1.032	0.927
	2021:W6	0.782	0.892	0.940	1.003	1.029	0.927
	2021:W7	0.779	0.887	0.941	1.004	1.042	0.926
	2021:W8	0.776	0.887	0.940	1.001	1.043	0.925
	2021:W9	0.703	0.779	0.855	0.954	0.988	0.851
	2021:W10	0.695	0.778	0.854	0.949	0.980	0.847
	2021:W11	0.688	0.771	0.853	0.942	0.979	0.843
	2021:W12	0.679	0.767	0.853	0.940	0.975	0.839
	2021:W13	0.621	0.651	0.796	0.888	0.937	0.779
	2021:W14	0.614	0.648	0.791	0.883	0.944	0.774
	2021:W15	0.608	0.644	0.787	0.877	0.943	0.769
	2021:W16	0.603	0.632	0.783	0.877	0.943	0.764
	2021:W17	0.550	0.583	0.728	0.834	0.925	0.719
	2021:W18	0.546	0.587	0.725	0.824	0.937	0.715
	2021:W19	0.543	0.589	0.724	0.824	0.946	0.710
	2021:W20	0.539	0.579	0.724	0.823	0.950	0.707
	2021:W21	0.472	0.571	0.682	0.803	0.908	0.678
	2021:W22	0.460	0.573	0.674	0.805	0.900	0.675
	2021:W23	0.454	0.575	0.660	0.805	0.901	0.672
	2021:W24	0.450	0.578	0.654	0.805	0.902	0.670
	2021:W25	0.499	0.578	0.659	0.787	0.897	0.668
	2021:W26	0.490	0.573	0.646	0.789	0.894	0.665
	2021:W27	0.482	0.573	0.644	0.789	0.890	0.662
	2021:W28	0.474	0.570	0.635	0.783	0.886	0.660
	2021:W29	0.434	0.547	0.630	0.777	0.868	0.642
	2021:W30	0.431	0.543	0.628	0.774	0.867	0.640
	2021:W31	0.429	0.538	0.627	0.770	0.869	0.639
	2021:W32	0.426	0.537	0.627	0.767	0.870	0.638
	2021:W33	0.409	0.514	0.653	0.804	0.871	0.646
	2021:W34	0.406	0.513	0.650	0.800	0.871	0.645
	2021:W35	0.402	0.512	0.649	0.797	0.872	0.644
	2021:W36	0.398	0.514	0.647	0.795	0.873	0.643
	2021:W37	0.375	0.502	0.638	0.771	0.904	0.632
	2021:W38	0.377	0.499	0.633	0.768	0.903	0.631
	2021:W39	0.379	0.495	0.630	0.766	0.901	0.630
	2021:W40	0.377	0.493	0.632	0.764	0.898	0.629
	2021:W41	0.377	0.479	0.639	0.738	0.928	0.623
	2021:W42	0.379	0.478	0.639	0.739	0.927	0.622
	2021:W43	0.380	0.481	0.643	0.750	0.926	0.623
	2021:W44	0.382	0.483	0.641	0.760	0.925	0.624
	2021:W45	0.381	0.465	0.628	0.754	0.895	0.612
	2021:W46	0.380	0.467	0.629	0.754	0.895	0.612
	2021:W47	0.378	0.468	0.625	0.757	0.893	0.611
	2021:W48	0.377	0.465	0.621	0.757	0.889	0.609

Note: The dependent variable is the state-level EC growth.

Table A3: Distribution of relative RMSFE across states for AR-W-M-Q model

Calendar (v)		10%	25%	50%	75%	90%	RMSE
Backcast	2021:W1	0.345	0.445	0.560	0.678	0.856	0.581
	2021:W2	0.355	0.445	0.557	0.679	0.863	0.579
	2021:W3	0.351	0.446	0.553	0.679	0.872	0.577
	2021:W4	0.354	0.439	0.548	0.676	0.886	0.576
Nowcast	2021:W5	0.824	0.906	0.968	1.045	1.173	0.963
	2021:W6	0.819	0.901	0.966	1.044	1.173	0.961
	2021:W7	0.811	0.896	0.965	1.041	1.172	0.959
	2021:W8	0.805	0.890	0.965	1.041	1.167	0.956
	2021:W9	0.698	0.770	0.878	0.965	1.061	0.868
	2021:W10	0.694	0.763	0.867	0.959	1.049	0.864
	2021:W11	0.689	0.760	0.857	0.953	1.037	0.860
	2021:W12	0.686	0.756	0.846	0.955	1.035	0.856
	2021:W13	0.640	0.694	0.815	0.909	1.031	0.807
	2021:W14	0.637	0.687	0.806	0.905	1.032	0.802
	2021:W15	0.628	0.680	0.798	0.901	1.032	0.798
	2021:W16	0.611	0.675	0.784	0.899	1.032	0.794
	2021:W17	0.566	0.636	0.739	0.841	1.004	0.745
	2021:W18	0.561	0.633	0.736	0.834	1.004	0.743
	2021:W19	0.556	0.631	0.733	0.829	1.002	0.741
	2021:W20	0.552	0.632	0.733	0.830	1.000	0.741
	2021:W21	0.519	0.622	0.732	0.818	0.950	0.716
	2021:W22	0.515	0.621	0.726	0.814	0.951	0.714
	2021:W23	0.508	0.616	0.715	0.812	0.953	0.711
	2021:W24	0.501	0.608	0.702	0.813	0.953	0.709
	2021:W25	0.517	0.597	0.718	0.814	0.963	0.714
	2021:W26	0.511	0.597	0.710	0.815	0.969	0.710
	2021:W27	0.506	0.597	0.703	0.816	0.971	0.708
	2021:W28	0.498	0.598	0.699	0.815	0.965	0.706
	2021:W29	0.439	0.570	0.692	0.808	0.928	0.689
	2021:W30	0.434	0.571	0.694	0.809	0.921	0.687
	2021:W31	0.429	0.567	0.699	0.808	0.917	0.685
	2021:W32	0.426	0.565	0.703	0.808	0.918	0.684
	2021:W33	0.422	0.552	0.683	0.845	0.907	0.681
	2021:W34	0.417	0.549	0.679	0.839	0.907	0.679
	2021:W35	0.411	0.549	0.676	0.834	0.906	0.677
	2021:W36	0.406	0.548	0.671	0.829	0.905	0.675
	2021:W37	0.405	0.530	0.683	0.803	0.938	0.666
	2021:W38	0.408	0.525	0.676	0.799	0.935	0.664
	2021:W39	0.407	0.520	0.669	0.796	0.929	0.661
	2021:W40	0.406	0.517	0.660	0.793	0.923	0.659
	2021:W41	0.407	0.508	0.658	0.773	0.954	0.648
	2021:W42	0.403	0.506	0.655	0.776	0.950	0.647
	2021:W43	0.402	0.507	0.655	0.779	0.948	0.648
	2021:W44	0.400	0.507	0.657	0.784	0.947	0.649
	2021:W45	0.374	0.468	0.594	0.737	0.922	0.599
	2021:W46	0.374	0.470	0.597	0.744	0.923	0.600
	2021:W47	0.373	0.469	0.599	0.743	0.922	0.600
	2021:W48	0.372	0.467	0.599	0.741	0.918	0.599

Note: The dependent variable is the state-level EC growth.

Table A4: Distribution of relative RMSFE across states for AR-M model

Calendar (v)		10%	25%	50%	75%	90%	RMSE
Backcast	2021:W1	0.410	0.482	0.629	0.751	0.872	0.622
	2021:W2	0.410	0.482	0.629	0.751	0.872	0.622
	2021:W3	0.410	0.482	0.629	0.751	0.872	0.622
	2021:W4	0.410	0.482	0.629	0.751	0.872	0.622
Nowcast	2021:W5	0.773	0.884	0.937	0.986	1.030	0.918
	2021:W6	0.773	0.884	0.937	0.986	1.030	0.918
	2021:W7	0.773	0.884	0.937	0.986	1.030	0.918
	2021:W8	0.773	0.884	0.937	0.986	1.030	0.918
	2021:W9	0.692	0.771	0.856	0.947	0.991	0.846
	2021:W10	0.692	0.771	0.856	0.947	0.991	0.846
	2021:W11	0.692	0.771	0.856	0.947	0.991	0.846
	2021:W12	0.692	0.771	0.856	0.947	0.991	0.846
	2021:W13	0.616	0.677	0.825	0.908	0.957	0.789
	2021:W14	0.616	0.677	0.825	0.908	0.957	0.789
	2021:W15	0.616	0.677	0.825	0.908	0.957	0.789
	2021:W16	0.616	0.677	0.825	0.908	0.957	0.789
	2021:W17	0.556	0.616	0.763	0.864	0.932	0.748
	2021:W18	0.556	0.616	0.763	0.864	0.932	0.748
	2021:W19	0.556	0.616	0.763	0.864	0.932	0.748
	2021:W20	0.556	0.616	0.763	0.864	0.932	0.748
	2021:W21	0.511	0.588	0.722	0.820	0.904	0.708
	2021:W22	0.511	0.588	0.722	0.820	0.904	0.708
	2021:W23	0.511	0.588	0.722	0.820	0.904	0.708
	2021:W24	0.511	0.588	0.722	0.820	0.904	0.708
	2021:W25	0.530	0.592	0.718	0.829	0.892	0.704
	2021:W26	0.530	0.592	0.718	0.829	0.892	0.704
	2021:W27	0.530	0.592	0.718	0.829	0.892	0.704
	2021:W28	0.530	0.592	0.718	0.829	0.892	0.704
	2021:W29	0.502	0.531	0.675	0.800	0.874	0.672
	2021:W30	0.502	0.531	0.675	0.800	0.874	0.672
	2021:W31	0.502	0.531	0.675	0.800	0.874	0.672
	2021:W32	0.502	0.531	0.675	0.800	0.874	0.672
	2021:W33	0.461	0.542	0.681	0.787	0.885	0.663
	2021:W34	0.461	0.542	0.681	0.787	0.885	0.663
	2021:W35	0.461	0.542	0.681	0.787	0.885	0.663
	2021:W36	0.461	0.542	0.681	0.787	0.885	0.663
	2021:W37	0.461	0.521	0.668	0.765	0.869	0.654
	2021:W38	0.461	0.521	0.668	0.765	0.869	0.654
	2021:W39	0.461	0.521	0.668	0.765	0.869	0.654
	2021:W40	0.461	0.521	0.668	0.765	0.869	0.654
	2021:W41	0.441	0.477	0.678	0.767	0.906	0.644
	2021:W42	0.441	0.477	0.678	0.767	0.906	0.644
	2021:W43	0.441	0.477	0.678	0.767	0.906	0.644
	2021:W44	0.441	0.477	0.678	0.767	0.906	0.644
	2021:W45	0.424	0.471	0.685	0.746	0.908	0.635
	2021:W46	0.424	0.471	0.685	0.746	0.908	0.635
	2021:W47	0.424	0.471	0.685	0.746	0.908	0.635
	2021:W48	0.424	0.471	0.685	0.746	0.908	0.635

Note: The dependent variable is the state-level EC growth.

Table A5: Distribution of relative RMSFE across states for AR-Q model

Calendar (v)		10%	25%	50%	75%	90%	RMSE
Backcast	2021:W1	0.657	0.761	0.887	0.950	0.986	0.845
	2021:W2	0.657	0.761	0.887	0.950	0.986	0.845
	2021:W3	0.657	0.761	0.887	0.950	0.986	0.845
	2021:W4	0.657	0.761	0.887	0.950	0.986	0.845
Nowcast	2021:W5	0.751	0.861	0.946	1.017	1.090	0.934
	2021:W6	0.751	0.861	0.946	1.017	1.090	0.934
	2021:W7	0.751	0.861	0.946	1.017	1.090	0.934
	2021:W8	0.751	0.861	0.946	1.017	1.090	0.934
	2021:W9	0.700	0.825	0.921	1.002	1.047	0.911
	2021:W10	0.700	0.825	0.921	1.002	1.047	0.911
	2021:W11	0.700	0.825	0.921	1.002	1.047	0.911
	2021:W12	0.700	0.825	0.921	1.002	1.047	0.911
	2021:W13	0.700	0.825	0.921	1.002	1.047	0.911
	2021:W14	0.700	0.825	0.921	1.002	1.047	0.911
	2021:W15	0.700	0.825	0.921	1.002	1.047	0.911
	2021:W16	0.700	0.825	0.921	1.002	1.047	0.911
	2021:W17	0.700	0.825	0.921	1.002	1.047	0.911
	2021:W18	0.700	0.825	0.921	1.002	1.047	0.911
	2021:W19	0.700	0.825	0.921	1.002	1.047	0.911
	2021:W20	0.700	0.825	0.921	1.002	1.047	0.911
	2021:W21	0.831	0.877	0.961	1.009	1.097	0.947
	2021:W22	0.831	0.877	0.961	1.009	1.097	0.947
	2021:W23	0.831	0.877	0.961	1.009	1.097	0.947
	2021:W24	0.831	0.877	0.961	1.009	1.097	0.947
	2021:W25	0.831	0.877	0.961	1.009	1.097	0.947
	2021:W26	0.831	0.877	0.961	1.009	1.097	0.947
	2021:W27	0.831	0.877	0.961	1.009	1.097	0.947
	2021:W28	0.831	0.877	0.961	1.009	1.097	0.947
	2021:W29	0.831	0.877	0.961	1.009	1.097	0.947
	2021:W30	0.831	0.877	0.961	1.009	1.097	0.947
	2021:W31	0.831	0.877	0.961	1.009	1.097	0.947
	2021:W32	0.831	0.877	0.961	1.009	1.097	0.947
	2021:W33	0.705	0.792	0.911	0.949	1.028	0.874
	2021:W34	0.705	0.792	0.911	0.949	1.028	0.874
	2021:W35	0.705	0.792	0.911	0.949	1.028	0.874
	2021:W36	0.705	0.792	0.911	0.949	1.028	0.874
	2021:W37	0.705	0.792	0.911	0.949	1.028	0.874
	2021:W38	0.705	0.792	0.911	0.949	1.028	0.874
	2021:W39	0.705	0.792	0.911	0.949	1.028	0.874
	2021:W40	0.705	0.792	0.911	0.949	1.028	0.874
	2021:W41	0.705	0.792	0.911	0.949	1.028	0.874
	2021:W42	0.705	0.792	0.911	0.949	1.028	0.874
	2021:W43	0.705	0.792	0.911	0.949	1.028	0.874
	2021:W44	0.705	0.792	0.911	0.949	1.028	0.874
	2021:W45	0.666	0.762	0.878	0.927	0.978	0.836
	2021:W46	0.666	0.762	0.878	0.927	0.978	0.836
	2021:W47	0.666	0.762	0.878	0.927	0.978	0.836
	2021:W48	0.666	0.762	0.878	0.927	0.978	0.836

Note: The dependent variable is the state-level EC growth.

Table A6: Distribution of relative RMSFE across states for AR model

Calendar (v)		10%	25%	50%	75%	90%	RMSE
Backcast	2021:W1	0.779	0.853	0.940	0.990	1.039	0.913
	2021:W2	0.779	0.853	0.940	0.990	1.039	0.913
	2021:W3	0.779	0.853	0.940	0.990	1.039	0.913
	2021:W4	0.779	0.853	0.940	0.990	1.039	0.913
Nowcast	2021:W5	0.806	0.864	0.949	0.979	1.015	0.918
	2021:W6	0.806	0.864	0.949	0.979	1.015	0.918
	2021:W7	0.806	0.864	0.949	0.979	1.015	0.918
	2021:W8	0.806	0.864	0.949	0.979	1.015	0.918
	2021:W9	0.806	0.864	0.949	0.979	1.015	0.918
	2021:W10	0.806	0.864	0.949	0.979	1.015	0.918
	2021:W11	0.806	0.864	0.949	0.979	1.015	0.918
	2021:W12	0.806	0.864	0.949	0.979	1.015	0.918
	2021:W13	0.806	0.864	0.949	0.979	1.015	0.918
	2021:W14	0.806	0.864	0.949	0.979	1.015	0.918
	2021:W15	0.806	0.864	0.949	0.979	1.015	0.918
	2021:W16	0.806	0.864	0.949	0.979	1.015	0.918
	2021:W17	0.806	0.864	0.949	0.979	1.015	0.918
	2021:W18	0.806	0.864	0.949	0.979	1.015	0.918
	2021:W19	0.806	0.864	0.949	0.979	1.015	0.918
	2021:W20	0.806	0.864	0.949	0.979	1.015	0.918
	2021:W21	0.812	0.881	0.955	0.986	1.013	0.924
	2021:W22	0.812	0.881	0.955	0.986	1.013	0.924
	2021:W23	0.812	0.881	0.955	0.986	1.013	0.924
	2021:W24	0.812	0.881	0.955	0.986	1.013	0.924
	2021:W25	0.812	0.881	0.955	0.986	1.013	0.924
	2021:W26	0.812	0.881	0.955	0.986	1.013	0.924
	2021:W27	0.812	0.881	0.955	0.986	1.013	0.924
	2021:W28	0.812	0.881	0.955	0.986	1.013	0.924
	2021:W29	0.812	0.881	0.955	0.986	1.013	0.924
	2021:W30	0.812	0.881	0.955	0.986	1.013	0.924
	2021:W31	0.812	0.881	0.955	0.986	1.013	0.924
	2021:W32	0.812	0.881	0.955	0.986	1.013	0.924
	2021:W33	0.812	0.881	0.955	0.986	1.013	0.924
	2021:W34	0.812	0.881	0.955	0.986	1.013	0.924
	2021:W35	0.812	0.881	0.955	0.986	1.013	0.924
	2021:W36	0.812	0.881	0.955	0.986	1.013	0.924
	2021:W37	0.812	0.881	0.955	0.986	1.013	0.924
	2021:W38	0.812	0.881	0.955	0.986	1.013	0.924
	2021:W39	0.812	0.881	0.955	0.986	1.013	0.924
	2021:W40	0.812	0.881	0.955	0.986	1.013	0.924
	2021:W41	0.812	0.881	0.955	0.986	1.013	0.924
	2021:W42	0.812	0.881	0.955	0.986	1.013	0.924
	2021:W43	0.812	0.881	0.955	0.986	1.013	0.924
	2021:W44	0.812	0.881	0.955	0.986	1.013	0.924
	2021:W45	0.812	0.881	0.955	0.986	1.013	0.924
	2021:W46	0.812	0.881	0.955	0.986	1.013	0.924
	2021:W47	0.812	0.881	0.955	0.986	1.013	0.924
	2021:W48	0.812	0.881	0.955	0.986	1.013	0.924

Note: The dependent variable is the state-level EC growth.

A.2 Supplementary tables for the out-of-sample nowcast of the growth rate of per-capita energy consumption

This Appendix provides supplementary tables detailing the quantiles of the distribution of the relative RMSFE across states for the additional models proposed to nowcast the growth rate of per-capita energy consumption.

Table A7: Distribution of relative RMSFE across states for AR-W model

Calendar (v)		10%	25%	50%	75%	90%	RMSE
Backcast	2021:W1	0.679	0.703	0.776	0.914	0.977	0.810
	2021:W2	0.677	0.701	0.773	0.909	0.972	0.805
	2021:W3	0.672	0.697	0.771	0.901	0.971	0.802
	2021:W4	0.651	0.678	0.756	0.886	0.984	0.791
Nowcast	2021:W5	0.871	0.934	0.982	1.016	1.051	0.966
	2021:W6	0.871	0.934	0.986	1.015	1.052	0.967
	2021:W7	0.869	0.939	0.989	1.019	1.053	0.968
	2021:W8	0.868	0.941	0.987	1.016	1.051	0.968
	2021:W9	0.867	0.941	0.987	1.014	1.052	0.967
	2021:W10	0.866	0.939	0.984	1.014	1.047	0.964
	2021:W11	0.865	0.934	0.977	1.013	1.040	0.961
	2021:W12	0.858	0.928	0.972	1.011	1.033	0.957
	2021:W13	0.857	0.924	0.967	1.007	1.026	0.954
	2021:W14	0.856	0.916	0.958	1.001	1.024	0.949
	2021:W15	0.854	0.912	0.952	0.990	1.024	0.945
	2021:W16	0.848	0.909	0.949	0.982	1.025	0.941
	2021:W17	0.841	0.906	0.944	0.976	1.024	0.936
	2021:W18	0.837	0.901	0.940	0.973	1.021	0.932
	2021:W19	0.832	0.893	0.937	0.971	1.020	0.927
	2021:W20	0.827	0.885	0.935	0.972	1.020	0.923
	2021:W21	0.810	0.879	0.937	0.972	1.028	0.923
	2021:W22	0.805	0.873	0.935	0.967	1.027	0.919
	2021:W23	0.799	0.872	0.926	0.965	1.026	0.916
	2021:W24	0.794	0.863	0.918	0.971	1.024	0.912
	2021:W25	0.789	0.858	0.914	0.963	1.028	0.907
	2021:W26	0.785	0.844	0.906	0.957	1.034	0.900
	2021:W27	0.791	0.838	0.892	0.950	1.033	0.895
	2021:W28	0.791	0.833	0.880	0.949	1.032	0.891
	2021:W29	0.786	0.830	0.874	0.955	1.031	0.888
	2021:W30	0.779	0.822	0.866	0.954	1.029	0.883
	2021:W31	0.770	0.820	0.861	0.958	1.027	0.882
	2021:W32	0.767	0.812	0.857	0.952	1.025	0.880
	2021:W33	0.764	0.810	0.859	0.949	1.022	0.878
	2021:W34	0.758	0.808	0.868	0.952	1.029	0.877
	2021:W35	0.752	0.802	0.878	0.955	1.045	0.877
	2021:W36	0.748	0.794	0.885	0.959	1.061	0.876
	2021:W37	0.745	0.785	0.887	0.960	1.062	0.875
	2021:W38	0.744	0.775	0.883	0.955	1.060	0.873
	2021:W39	0.746	0.767	0.883	0.952	1.056	0.871
	2021:W40	0.746	0.762	0.887	0.948	1.052	0.870
	2021:W41	0.745	0.760	0.892	0.947	1.048	0.869
	2021:W42	0.749	0.761	0.889	0.945	1.045	0.868
	2021:W43	0.744	0.762	0.883	0.947	1.046	0.868
	2021:W44	0.744	0.762	0.871	0.947	1.049	0.867
	2021:W45	0.739	0.764	0.861	0.948	1.049	0.866
	2021:W46	0.737	0.766	0.858	0.944	1.046	0.865
	2021:W47	0.733	0.766	0.856	0.938	1.043	0.863
	2021:W48	0.729	0.765	0.857	0.940	1.042	0.859

Note: The dependent variables is the state-level EC per capita growth.

Table A8: Distribution of relative RMSFE across states for AR-W-M model

Calendar (v)		10%	25%	50%	75%	90%	RMSE
Backcast	2021:W1	0.407	0.453	0.620	0.752	0.926	0.627
	2021:W2	0.404	0.448	0.610	0.752	0.922	0.625
	2021:W3	0.399	0.449	0.605	0.752	0.930	0.623
	2021:W4	0.393	0.453	0.604	0.750	0.932	0.622
Nowcast	2021:W5	0.892	0.919	0.966	1.016	1.050	0.961
	2021:W6	0.897	0.920	0.964	1.014	1.046	0.962
	2021:W7	0.898	0.926	0.963	1.013	1.044	0.962
	2021:W8	0.895	0.926	0.966	1.011	1.039	0.961
	2021:W9	0.772	0.833	0.897	0.961	1.002	0.888
	2021:W10	0.770	0.832	0.894	0.960	0.999	0.885
	2021:W11	0.767	0.829	0.899	0.956	0.999	0.882
	2021:W12	0.764	0.822	0.891	0.949	0.994	0.878
	2021:W13	0.652	0.740	0.843	0.909	0.979	0.825
	2021:W14	0.646	0.730	0.839	0.902	0.976	0.821
	2021:W15	0.641	0.720	0.836	0.902	0.974	0.817
	2021:W16	0.634	0.709	0.830	0.899	0.974	0.812
	2021:W17	0.592	0.662	0.797	0.850	0.954	0.773
	2021:W18	0.587	0.657	0.791	0.845	0.950	0.769
	2021:W19	0.582	0.655	0.786	0.844	0.955	0.766
	2021:W20	0.577	0.655	0.782	0.845	0.955	0.763
	2021:W21	0.532	0.615	0.731	0.824	0.929	0.724
	2021:W22	0.522	0.616	0.722	0.819	0.935	0.720
	2021:W23	0.512	0.614	0.712	0.822	0.939	0.717
	2021:W24	0.504	0.612	0.702	0.825	0.945	0.714
	2021:W25	0.513	0.644	0.717	0.821	0.915	0.716
	2021:W26	0.512	0.637	0.706	0.821	0.921	0.711
	2021:W27	0.514	0.632	0.699	0.821	0.929	0.708
	2021:W28	0.517	0.627	0.691	0.821	0.937	0.705
	2021:W29	0.492	0.605	0.694	0.813	0.953	0.693
	2021:W30	0.488	0.605	0.685	0.808	0.955	0.691
	2021:W31	0.485	0.601	0.683	0.806	0.948	0.689
	2021:W32	0.482	0.593	0.679	0.803	0.944	0.687
	2021:W33	0.482	0.569	0.703	0.817	0.928	0.690
	2021:W34	0.483	0.568	0.702	0.818	0.928	0.689
	2021:W35	0.484	0.567	0.699	0.818	0.929	0.688
	2021:W36	0.484	0.565	0.695	0.813	0.930	0.687
	2021:W37	0.467	0.553	0.679	0.794	0.925	0.682
	2021:W38	0.468	0.552	0.675	0.791	0.943	0.680
	2021:W39	0.469	0.547	0.672	0.787	0.947	0.679
	2021:W40	0.468	0.544	0.669	0.783	0.950	0.677
	2021:W41	0.425	0.532	0.669	0.785	0.999	0.672
	2021:W42	0.424	0.532	0.671	0.788	1.001	0.671
	2021:W43	0.424	0.532	0.669	0.793	0.998	0.671
	2021:W44	0.424	0.532	0.667	0.798	0.998	0.671
	2021:W45	0.402	0.515	0.680	0.793	0.981	0.661
	2021:W46	0.403	0.514	0.681	0.804	0.983	0.661
	2021:W47	0.403	0.511	0.677	0.809	0.986	0.659
	2021:W48	0.404	0.507	0.676	0.807	0.985	0.657

Note: The dependent variable is the state-level EC per capita growth.

Table A9: Distribution of relative RMSFE across states for AR-M model

Calendar (v)		10%	25%	50%	75%	90%	RMSE
Backcast	2021:W1	0.469	0.528	0.688	0.832	0.944	0.684
	2021:W2	0.469	0.528	0.688	0.832	0.944	0.684
	2021:W3	0.469	0.528	0.688	0.832	0.944	0.684
	2021:W4	0.469	0.528	0.688	0.832	0.944	0.684
Nowcast	2021:W5	0.877	0.913	0.954	0.991	1.031	0.950
	2021:W6	0.877	0.913	0.954	0.991	1.031	0.950
	2021:W7	0.877	0.913	0.954	0.991	1.031	0.950
	2021:W8	0.877	0.913	0.954	0.991	1.031	0.950
	2021:W9	0.773	0.817	0.874	0.957	0.988	0.877
	2021:W10	0.773	0.817	0.874	0.957	0.988	0.877
	2021:W11	0.773	0.817	0.874	0.957	0.988	0.877
	2021:W12	0.773	0.817	0.874	0.957	0.988	0.877
	2021:W13	0.652	0.735	0.861	0.905	0.985	0.826
	2021:W14	0.652	0.735	0.861	0.905	0.985	0.826
	2021:W15	0.652	0.735	0.861	0.905	0.985	0.826
	2021:W16	0.652	0.735	0.861	0.905	0.985	0.826
	2021:W17	0.609	0.680	0.807	0.884	0.956	0.789
	2021:W18	0.609	0.680	0.807	0.884	0.956	0.789
	2021:W19	0.609	0.680	0.807	0.884	0.956	0.789
	2021:W20	0.609	0.680	0.807	0.884	0.956	0.789
	2021:W21	0.542	0.664	0.750	0.853	0.913	0.747
	2021:W22	0.542	0.664	0.750	0.853	0.913	0.747
	2021:W23	0.542	0.664	0.750	0.853	0.913	0.747
	2021:W24	0.542	0.664	0.750	0.853	0.913	0.747
	2021:W25	0.541	0.656	0.753	0.850	0.899	0.743
	2021:W26	0.541	0.656	0.753	0.850	0.899	0.743
	2021:W27	0.541	0.656	0.753	0.850	0.899	0.743
	2021:W28	0.541	0.656	0.753	0.850	0.899	0.743
	2021:W29	0.521	0.644	0.733	0.823	0.904	0.718
	2021:W30	0.521	0.644	0.733	0.823	0.904	0.718
	2021:W31	0.521	0.644	0.733	0.823	0.904	0.718
	2021:W32	0.521	0.644	0.733	0.823	0.904	0.718
	2021:W33	0.519	0.598	0.756	0.811	0.946	0.713
	2021:W34	0.519	0.598	0.756	0.811	0.946	0.713
	2021:W35	0.519	0.598	0.756	0.811	0.946	0.713
	2021:W36	0.519	0.598	0.756	0.811	0.946	0.713
	2021:W37	0.509	0.614	0.730	0.800	0.933	0.706
	2021:W38	0.509	0.614	0.730	0.800	0.933	0.706
	2021:W39	0.509	0.614	0.730	0.800	0.933	0.706
	2021:W40	0.509	0.614	0.730	0.800	0.933	0.706
	2021:W41	0.476	0.567	0.720	0.824	0.935	0.701
	2021:W42	0.476	0.567	0.720	0.824	0.935	0.701
	2021:W43	0.476	0.567	0.720	0.824	0.935	0.701
	2021:W44	0.476	0.567	0.720	0.824	0.935	0.701
	2021:W45	0.468	0.558	0.710	0.819	0.933	0.696
	2021:W46	0.468	0.558	0.710	0.819	0.933	0.696
	2021:W47	0.468	0.558	0.710	0.819	0.933	0.696
	2021:W48	0.468	0.558	0.710	0.819	0.933	0.696

Note: The dependent variable is the state-level EC per capita growth.

Table A10: Distribution of relative RMSFE across states for AR-Q model

Calendar (v)		10%	25%	50%	75%	90%	RMSE
Backcast	2021:W1	0.759	0.836	0.908	0.965	0.991	0.892
	2021:W2	0.759	0.836	0.908	0.965	0.991	0.892
	2021:W3	0.759	0.836	0.908	0.965	0.991	0.892
	2021:W4	0.759	0.836	0.908	0.965	0.991	0.892
Nowcast	2021:W5	0.782	0.888	0.944	1.016	1.131	0.950
	2021:W6	0.782	0.888	0.944	1.016	1.131	0.950
	2021:W7	0.782	0.888	0.944	1.016	1.131	0.950
	2021:W8	0.782	0.888	0.944	1.016	1.131	0.950
	2021:W9	0.768	0.865	0.920	1.001	1.081	0.930
	2021:W10	0.768	0.865	0.920	1.001	1.081	0.930
	2021:W11	0.768	0.865	0.920	1.001	1.081	0.930
	2021:W12	0.768	0.865	0.920	1.001	1.081	0.930
	2021:W13	0.768	0.865	0.920	1.001	1.081	0.930
	2021:W14	0.768	0.865	0.920	1.001	1.081	0.930
	2021:W15	0.768	0.865	0.920	1.001	1.081	0.930
	2021:W16	0.768	0.865	0.920	1.001	1.081	0.930
	2021:W17	0.768	0.865	0.920	1.001	1.081	0.930
	2021:W18	0.768	0.865	0.920	1.001	1.081	0.930
	2021:W19	0.768	0.865	0.920	1.001	1.081	0.930
	2021:W20	0.768	0.865	0.920	1.001	1.081	0.930
	2021:W21	0.854	0.914	0.971	1.001	1.064	0.954
	2021:W22	0.854	0.914	0.971	1.001	1.064	0.954
	2021:W23	0.854	0.914	0.971	1.001	1.064	0.954
	2021:W24	0.854	0.914	0.971	1.001	1.064	0.954
	2021:W25	0.854	0.914	0.971	1.001	1.064	0.954
	2021:W26	0.854	0.914	0.971	1.001	1.064	0.954
	2021:W27	0.854	0.914	0.971	1.001	1.064	0.954
	2021:W28	0.854	0.914	0.971	1.001	1.064	0.954
	2021:W29	0.854	0.914	0.971	1.001	1.064	0.954
	2021:W30	0.854	0.914	0.971	1.001	1.064	0.954
	2021:W31	0.854	0.914	0.971	1.001	1.064	0.954
	2021:W32	0.854	0.914	0.971	1.001	1.064	0.954
	2021:W33	0.792	0.847	0.917	0.958	1.002	0.906
	2021:W34	0.792	0.847	0.917	0.958	1.002	0.906
	2021:W35	0.792	0.847	0.917	0.958	1.002	0.906
	2021:W36	0.792	0.847	0.917	0.958	1.002	0.906
	2021:W37	0.792	0.847	0.917	0.958	1.002	0.906
	2021:W38	0.792	0.847	0.917	0.958	1.002	0.906
	2021:W39	0.792	0.847	0.917	0.958	1.002	0.906
	2021:W40	0.792	0.847	0.917	0.958	1.002	0.906
	2021:W41	0.792	0.847	0.917	0.958	1.002	0.906
	2021:W42	0.792	0.847	0.917	0.958	1.002	0.906
	2021:W43	0.792	0.847	0.917	0.958	1.002	0.906
	2021:W44	0.792	0.847	0.917	0.958	1.002	0.906
	2021:W45	0.756	0.819	0.894	0.962	0.996	0.887
	2021:W46	0.756	0.819	0.894	0.962	0.996	0.887
	2021:W47	0.756	0.819	0.894	0.962	0.996	0.887
	2021:W48	0.756	0.819	0.894	0.962	0.996	0.887

Note: The dependent variable is the state-level EC per capita growth.

Table A11: Distribution of relative RMSFE across states for AR model

Calendar (v)		10%	25%	50%	75%	90%	RMSE
Backcast	2021:W1	0.846	0.892	0.957	0.983	1.002	0.929
	2021:W2	0.846	0.892	0.957	0.983	1.002	0.929
	2021:W3	0.846	0.892	0.957	0.983	1.002	0.929
	2021:W4	0.846	0.892	0.957	0.983	1.002	0.929
Nowcast	2021:W5	0.872	0.926	0.966	0.994	1.007	0.952
	2021:W6	0.872	0.926	0.966	0.994	1.007	0.952
	2021:W7	0.872	0.926	0.966	0.994	1.007	0.952
	2021:W8	0.872	0.926	0.966	0.994	1.007	0.952
	2021:W9	0.872	0.926	0.966	0.994	1.007	0.952
	2021:W10	0.872	0.926	0.966	0.994	1.007	0.952
	2021:W11	0.872	0.926	0.966	0.994	1.007	0.952
	2021:W12	0.872	0.926	0.966	0.994	1.007	0.952
	2021:W13	0.872	0.926	0.966	0.994	1.007	0.952
	2021:W14	0.872	0.926	0.966	0.994	1.007	0.952
	2021:W15	0.872	0.926	0.966	0.994	1.007	0.952
	2021:W16	0.872	0.926	0.966	0.994	1.007	0.952
	2021:W17	0.872	0.926	0.966	0.994	1.007	0.952
	2021:W18	0.872	0.926	0.966	0.994	1.007	0.952
	2021:W19	0.872	0.926	0.966	0.994	1.007	0.952
	2021:W20	0.872	0.926	0.966	0.994	1.007	0.952
	2021:W21	0.867	0.921	0.950	0.990	1.016	0.944
	2021:W22	0.867	0.921	0.950	0.990	1.016	0.944
	2021:W23	0.867	0.921	0.950	0.990	1.016	0.944
	2021:W24	0.867	0.921	0.950	0.990	1.016	0.944
	2021:W25	0.867	0.921	0.950	0.990	1.016	0.944
	2021:W26	0.867	0.921	0.950	0.990	1.016	0.944
	2021:W27	0.867	0.921	0.950	0.990	1.016	0.944
	2021:W28	0.867	0.921	0.950	0.990	1.016	0.944
	2021:W29	0.867	0.921	0.950	0.990	1.016	0.944
	2021:W30	0.867	0.921	0.950	0.990	1.016	0.944
	2021:W31	0.867	0.921	0.950	0.990	1.016	0.944
	2021:W32	0.867	0.921	0.950	0.990	1.016	0.944
	2021:W33	0.867	0.921	0.950	0.990	1.016	0.944
	2021:W34	0.867	0.921	0.950	0.990	1.016	0.944
	2021:W35	0.867	0.921	0.950	0.990	1.016	0.944
	2021:W36	0.867	0.921	0.950	0.990	1.016	0.944
	2021:W37	0.867	0.921	0.950	0.990	1.016	0.944
	2021:W38	0.867	0.921	0.950	0.990	1.016	0.944
	2021:W39	0.867	0.921	0.950	0.990	1.016	0.944
	2021:W40	0.867	0.921	0.950	0.990	1.016	0.944
	2021:W41	0.867	0.921	0.950	0.990	1.016	0.944
	2021:W42	0.867	0.921	0.950	0.990	1.016	0.944
	2021:W43	0.867	0.921	0.950	0.990	1.016	0.944
	2021:W44	0.867	0.921	0.950	0.990	1.016	0.944
	2021:W45	0.867	0.921	0.950	0.990	1.016	0.944
	2021:W46	0.867	0.921	0.950	0.990	1.016	0.944
	2021:W47	0.867	0.921	0.950	0.990	1.016	0.944
	2021:W48	0.867	0.921	0.950	0.990	1.016	0.944

Note: The dependent variable is the state-level EC per capita growth.

A.3 Supplementary tables for the out-of-sample nowcast of the growth rate of per-capita CO2 emissions using the AR-W-M-Q model

This Appendix provides supplementary tables detailing the quantiles of the distribution of the relative QS across states for the AR-W-M-Q model, the model with the best performance in nowcasting the growth rate of per-capita CO2 emissions.

Table A12: Distribution of relative QS across states for AR-W-M-Q model, $\tau = 0.25$

Calendar (v)		10%	25%	50%	75%	90%	QS
Backcast	2021:W1	0.568	0.635	0.796	0.867	1.117	0.798
	2021:W2	0.568	0.636	0.797	0.862	1.110	0.796
	2021:W3	0.569	0.635	0.798	0.858	1.102	0.795
	2021:W4	0.572	0.634	0.793	0.857	1.091	0.794
Nowcast	2021:W5	0.778	0.901	1.036	1.165	1.395	1.061
	2021:W6	0.775	0.901	1.038	1.164	1.395	1.061
	2021:W7	0.771	0.902	1.042	1.167	1.394	1.061
	2021:W8	0.769	0.903	1.046	1.170	1.391	1.060
	2021:W9	0.771	0.841	1.023	1.122	1.315	1.030
	2021:W10	0.768	0.840	1.023	1.124	1.311	1.027
	2021:W11	0.768	0.839	1.022	1.125	1.307	1.024
	2021:W12	0.768	0.837	1.021	1.130	1.302	1.021
	2021:W13	0.735	0.822	0.959	1.046	1.251	0.965
	2021:W14	0.732	0.820	0.954	1.041	1.246	0.961
	2021:W15	0.730	0.818	0.944	1.036	1.241	0.956
	2021:W16	0.728	0.814	0.933	1.030	1.237	0.952
	2021:W17	0.720	0.773	0.874	0.998	1.180	0.907
	2021:W18	0.718	0.767	0.874	0.999	1.176	0.904
	2021:W19	0.716	0.763	0.874	1.001	1.173	0.903
	2021:W20	0.714	0.759	0.873	1.004	1.174	0.902
	2021:W21	0.684	0.760	0.853	0.961	1.060	0.879
	2021:W22	0.681	0.757	0.849	0.961	1.059	0.876
	2021:W23	0.678	0.755	0.842	0.960	1.057	0.873
	2021:W24	0.676	0.752	0.836	0.959	1.056	0.870
	2021:W25	0.694	0.765	0.841	0.980	1.092	0.879
	2021:W26	0.688	0.758	0.831	0.978	1.087	0.875
	2021:W27	0.680	0.754	0.829	0.974	1.083	0.872
	2021:W28	0.681	0.741	0.827	0.971	1.078	0.868
	2021:W29	0.674	0.745	0.810	0.956	1.078	0.860
	2021:W30	0.667	0.735	0.805	0.957	1.088	0.858
	2021:W31	0.663	0.726	0.805	0.959	1.092	0.856
	2021:W32	0.659	0.716	0.805	0.959	1.091	0.854
	2021:W33	0.625	0.683	0.774	0.918	1.167	0.827
	2021:W34	0.629	0.678	0.769	0.915	1.161	0.826
	2021:W35	0.628	0.680	0.768	0.910	1.156	0.825
	2021:W36	0.625	0.688	0.769	0.902	1.150	0.823
	2021:W37	0.608	0.694	0.771	0.911	1.056	0.819
	2021:W38	0.606	0.687	0.768	0.906	1.052	0.816
	2021:W39	0.603	0.691	0.765	0.905	1.048	0.813
	2021:W40	0.600	0.691	0.761	0.905	1.044	0.810
	2021:W41	0.596	0.669	0.744	0.877	1.070	0.795
	2021:W42	0.592	0.669	0.743	0.874	1.067	0.793
	2021:W43	0.589	0.669	0.743	0.874	1.069	0.793
	2021:W44	0.586	0.668	0.743	0.874	1.069	0.793
	2021:W45	0.561	0.646	0.727	0.841	1.088	0.780
	2021:W46	0.567	0.644	0.723	0.842	1.086	0.780
	2021:W47	0.568	0.641	0.719	0.842	1.083	0.779
	2021:W48	0.567	0.638	0.716	0.844	1.075	0.778

Note: The dependent variable is the state-level CO2 per capita growth.

Table A13: Distribution of relative QS across states for AR-W-M-Q model, $\tau = 0.50$

	Calendar (v)	10%	25%	50%	75%	90%	QS
Backcast	2021:W1	0.628	0.662	0.754	0.870	0.966	0.779
	2021:W2	0.625	0.659	0.756	0.868	0.963	0.778
	2021:W3	0.621	0.660	0.756	0.868	0.962	0.777
	2021:W4	0.620	0.663	0.756	0.868	0.960	0.776
Nowcast	2021:W5	0.785	0.874	0.988	1.051	1.189	0.982
	2021:W6	0.783	0.876	0.986	1.052	1.189	0.982
	2021:W7	0.781	0.876	0.983	1.053	1.188	0.982
	2021:W8	0.778	0.878	0.982	1.054	1.186	0.981
	2021:W9	0.727	0.855	0.939	1.008	1.143	0.939
	2021:W10	0.723	0.856	0.938	1.001	1.144	0.937
	2021:W11	0.717	0.856	0.936	0.996	1.145	0.935
	2021:W12	0.714	0.852	0.933	0.994	1.144	0.933
	2021:W13	0.705	0.833	0.893	0.967	1.071	0.896
	2021:W14	0.702	0.831	0.887	0.964	1.071	0.893
	2021:W15	0.698	0.831	0.883	0.963	1.070	0.890
	2021:W16	0.693	0.832	0.878	0.962	1.069	0.888
	2021:W17	0.684	0.770	0.840	0.958	1.043	0.862
	2021:W18	0.681	0.772	0.841	0.957	1.045	0.861
	2021:W19	0.680	0.776	0.840	0.955	1.047	0.861
	2021:W20	0.680	0.777	0.839	0.958	1.050	0.861
	2021:W21	0.676	0.731	0.834	0.930	1.015	0.840
	2021:W22	0.669	0.730	0.836	0.927	1.016	0.838
	2021:W23	0.664	0.731	0.834	0.924	1.009	0.837
	2021:W24	0.661	0.727	0.831	0.924	1.016	0.836
	2021:W25	0.667	0.728	0.832	0.928	1.018	0.840
	2021:W26	0.663	0.725	0.829	0.928	1.018	0.838
	2021:W27	0.659	0.717	0.830	0.925	1.019	0.836
	2021:W28	0.656	0.710	0.829	0.919	1.018	0.835
	2021:W29	0.652	0.723	0.790	0.923	1.020	0.828
	2021:W30	0.650	0.718	0.786	0.920	1.026	0.826
	2021:W31	0.648	0.716	0.780	0.918	1.034	0.824
	2021:W32	0.645	0.714	0.776	0.913	1.039	0.823
	2021:W33	0.606	0.675	0.773	0.908	1.023	0.804
	2021:W34	0.612	0.678	0.770	0.905	1.024	0.803
	2021:W35	0.619	0.677	0.766	0.901	1.024	0.802
	2021:W36	0.621	0.674	0.765	0.896	1.024	0.801
	2021:W37	0.613	0.671	0.776	0.859	1.011	0.795
	2021:W38	0.610	0.664	0.776	0.856	1.013	0.793
	2021:W39	0.607	0.661	0.777	0.856	1.014	0.792
	2021:W40	0.605	0.662	0.776	0.857	1.016	0.790
	2021:W41	0.597	0.670	0.769	0.851	1.005	0.777
	2021:W42	0.595	0.672	0.767	0.849	1.002	0.776
	2021:W43	0.595	0.668	0.767	0.846	1.003	0.776
	2021:W44	0.595	0.667	0.766	0.843	1.002	0.776
	2021:W45	0.567	0.663	0.751	0.812	0.972	0.763
	2021:W46	0.568	0.660	0.749	0.812	0.973	0.763
	2021:W47	0.567	0.657	0.747	0.812	0.973	0.763
	2021:W48	0.566	0.653	0.746	0.811	0.972	0.762

Note: The dependent variable is the state-level CO2 per capita growth.

Table A14: Distribution of relative QS across states for AR-W-M-Q model, $\tau = 0.75$

	Calendar (v)	10%	25%	50%	75%	90%	QS
Backcast	2021:W1	0.544	0.694	0.771	0.896	1.036	0.792
	2021:W2	0.546	0.692	0.768	0.889	1.044	0.792
	2021:W3	0.549	0.688	0.769	0.885	1.047	0.792
	2021:W4	0.553	0.689	0.778	0.882	1.059	0.792
Nowcast	2021:W5	0.772	0.821	0.918	1.047	1.172	0.945
	2021:W6	0.773	0.823	0.920	1.048	1.170	0.945
	2021:W7	0.773	0.825	0.921	1.049	1.166	0.945
	2021:W8	0.770	0.826	0.922	1.051	1.165	0.945
	2021:W9	0.727	0.770	0.910	1.013	1.138	0.900
	2021:W10	0.725	0.769	0.911	1.011	1.140	0.899
	2021:W11	0.722	0.770	0.909	1.010	1.141	0.898
	2021:W12	0.719	0.769	0.901	1.010	1.144	0.896
	2021:W13	0.693	0.753	0.866	0.973	1.130	0.881
	2021:W14	0.690	0.750	0.862	0.971	1.127	0.879
	2021:W15	0.688	0.748	0.862	0.969	1.126	0.877
	2021:W16	0.685	0.746	0.863	0.966	1.126	0.876
	2021:W17	0.657	0.742	0.853	0.960	1.095	0.859
	2021:W18	0.654	0.742	0.856	0.960	1.090	0.858
	2021:W19	0.650	0.739	0.859	0.960	1.086	0.858
	2021:W20	0.650	0.737	0.861	0.957	1.083	0.858
	2021:W21	0.649	0.720	0.825	0.903	1.035	0.832
	2021:W22	0.648	0.723	0.820	0.904	1.036	0.831
	2021:W23	0.646	0.723	0.815	0.898	1.038	0.831
	2021:W24	0.644	0.722	0.813	0.895	1.039	0.830
	2021:W25	0.648	0.732	0.834	0.904	1.035	0.833
	2021:W26	0.645	0.730	0.829	0.912	1.039	0.832
	2021:W27	0.643	0.728	0.826	0.914	1.046	0.831
	2021:W28	0.640	0.726	0.821	0.912	1.054	0.830
	2021:W29	0.617	0.708	0.823	0.910	1.068	0.827
	2021:W30	0.614	0.703	0.821	0.910	1.067	0.824
	2021:W31	0.611	0.700	0.819	0.906	1.068	0.822
	2021:W32	0.611	0.697	0.816	0.904	1.065	0.821
	2021:W33	0.593	0.680	0.809	0.882	1.030	0.809
	2021:W34	0.591	0.679	0.813	0.884	1.029	0.808
	2021:W35	0.588	0.678	0.813	0.882	1.030	0.807
	2021:W36	0.585	0.677	0.813	0.880	1.030	0.806
	2021:W37	0.604	0.687	0.813	0.889	1.047	0.807
	2021:W38	0.602	0.688	0.810	0.887	1.044	0.806
	2021:W39	0.599	0.686	0.806	0.885	1.040	0.805
	2021:W40	0.596	0.686	0.802	0.883	1.036	0.804
	2021:W41	0.580	0.661	0.799	0.891	1.008	0.797
	2021:W42	0.581	0.661	0.797	0.889	1.005	0.796
	2021:W43	0.584	0.663	0.796	0.886	1.007	0.796
	2021:W44	0.588	0.665	0.795	0.883	1.007	0.796
	2021:W45	0.583	0.649	0.780	0.864	0.979	0.785
	2021:W46	0.584	0.648	0.783	0.864	0.977	0.785
	2021:W47	0.585	0.646	0.784	0.865	0.978	0.785
	2021:W48	0.586	0.644	0.785	0.864	0.978	0.785

Note: The dependent variable is the state-level CO2 per capita growth.